Master's thesis

NTNU
Norwegian University of Science and Technology
Faculty of Engineering
Department of Marine Technology

Helen Ege

Investigation of the Tower Design for the Offshore Wind Turbine Concept OO-Star Wind Floater

Master's thesis in Marine Technology
Supervisor: Jørgen Amdahl
June 2019

NTNU
Norwegian University of
Science and Technology

Helen Ege

Investigation of the Tower Design for the Offshore Wind Turbine Concept OO-Star Wind Floater

Master's thesis in Marine Technology
Supervisor: Jørgen Amdahl
June 2019

Norwegian University of Science and Technology
Faculty of Engineering
Department of Marine Technology

NTNU
Norwegian University of
Science and Technology

NTNU – Trondheim
Norwegian University of
Science and Technology

Investigation of the Tower Design for the Offshore Wind Turbine Concept OO-Star Wind Floater

Helen Ege

June 2019

MASTERS THESIS

Department of Marine Technology

Norwegian University of Science and Technology

Supervisor 1: Prof. Jørgen Amdahl

Supervisor 2: PhD student Stian Sørum

Contact person in Dr. Techn Olav Olsen: Håkon S. Andersen

Preface

This masters thesis is submitted to the Department of Marine Technology at the Norwegian University of Science and Technology. It was written during the spring semester of 2019. The thesis is a part of the study program Marine Structures and it is based on the offshore wind industry. The subject was chosen because of a personal interest in the industry and a desire to work on improving the structural design of an offshore wind turbine. The floating wind turbine concept OO-Star Wind Turbine is considered a realistic and innovating design, and it was very motivating to contribute to further optimization of the concept. The thesis is written with regards to an individual with relevant background and understanding in marine engineering.

The thesis is based on cooperation with the company Dr. Techn. Olav Olsen. Input has been provided on both content and model from Dr. Techn. Olav Olsen and SINTEF Ocean.

Helen Ege

Trondheim, 2019-06-11

NTNU
Norges teknisk-naturvitenskapelige universitet
Institutt for marin teknikk

MASTER THESIS 2019

For

Stud. Helen Ege

Analysis of the offshore wind turbine concept – OO Star Wind Floater
Analyse av offshore vindturbinkonspet- OO Star Wind Floater

Background;
Towers for floating wind turbines are subjected to significant fatigue due to wind and wave action. There is a need for optimizing the tower to reduce the cost of offshore wind floaters. Typically large floating wind turbines have been designed with a stiff-stiff tower. This will imply that the frequency of the first bending mode is above the 3P frequency. It is important to evaluate the required difference between the eigen frequency of the tower and the 3P frequency in order to avoid significant response. For bottom fixed the frequency of the first bending mode is typically located between 1P and 3P (soft-stiff). It could be interesting to evaluate a soft-stiff tower also for floating wind turbines as simulations indicate that this could be relevant for the OO-Star Wind Floater

Project main objective;
Evaluate the sensitivity of the tower design with respect to rotational frequencies of the turbine (1P, 3P, etc) for the OO-Star Wind Floater)

The following topics should be addressed:

1. Brief review of principles for analysis and design of offshore wind turbines and the challenges related to floating turbines.

2. Use an existing flexible tower model of the floater for analysis with SIMA. Include DTU turbine and controller (should be provided by OO/Sintef Ocean or through Lifes50+). Calibrate the potential theory model with flexible tower (RIFLEX-elements) above the still water line in SIMA to represent the correct eigenfrequency and verify that the mode shape is reasonable (possibly in collaboration with Daniel Kaasa). The element between

the water line and the steel tower flange should be tuned to provide the relevant eigen frequency.

3. Perform coupled, stochastic analysis of the tower based on simulation with SIMA for a set of representative environmental conditions (waves and wind) for long term fatigue damage assessment. Use SCFs and SN-curves relevant for design of tower.

4. Vary the stiffness of the tower so as to obtain desired eigenperiods. Discuss how this can be achieved in practise and perform a priori estimation of the impact it will have on the fatigue damage. Conduct simulations with SIMA as described in Pt.6.

5. For selected extreme environmental conditions determine characteristic values of blade tip clearance and utilization w.r.t. buckling /yielding of the tower. Use of the contour line method may be considered.

6. Conclusions and recommendations for further work

Input (from OO/Sintef Ocean):
- Public version of OO-Star Wind Floater as defined through the Lifes50+ project.
- DTU turbine and controller.
- Relevant documents from Lifes50+ and possibly other sources.

Literature studies of specific topics relevant to the thesis work may be included.

The work scope may prove to be larger than initially anticipated. Subject to approval from the supervisor, topics may be deleted from the list above or reduced in extent.

In the thesis the candidate shall present his personal contribution to the resolution of problems within the scope of the thesis work.

Theories and conclusions should be based on mathematical derivations and/or logic reasoning identifying the various steps in the deduction.

The candidate should utilize the existing possibilities for obtaining relevant literature.

The thesis should be organized in a rational manner to give a clear exposition of results, assessments, and conclusions. The text should be brief and to the point, with a clear language. Telegraphic language should be avoided.

The thesis shall contain the following elements: A text defining the scope, preface, list of contents, summary, main body of thesis, conclusions with recommendations for further work, list

of symbols and acronyms, references and (optional) appendices. All figures, tables and equations shall be numerated.

The supervisor may require that the candidate, in an early stage of the work, presents a written plan for the completion of the work. The plan should include a budget for the use of computer and laboratory resources which will be charged to the department. Overruns shall be reported to the supervisor.

The original contribution of the candidate and material taken from other sources shall be clearly defined. Work from other sources shall be properly referenced using an acknowledged referencing system.

The report shall be submitted in two copies:

- Signed by the candidate
- The text defining the scope included
- In bound volume(s)
- Drawings and/or computer prints which cannot be bound should be organised in a separate folder.

Supervisor:
Prof. Jørgen Amdahl

PhD student Stian Sørum

Contact person Olav Olsen
Håkon S. Andersen

Deadline: June 11 , 2019

Trondheim, January 25, 2019

Jørgen Amdahl

Acknowledgments

I would like to express gratefulness for input, discussions and help from company contacts and supervisors. First and foremost, I would like to thank my supervisors Jørgen Amdahl and Stian Sørum for the conversations around the topic and the input on ways to solve the objectives. Special thanks are appropriate to give Stian Sørum for the help and guidance in use of the software, and because of the extraordinary willingness to help on a minute notice. In addition, I would like to thank Associate Prof. Erin Bachynski for the helpful and necessary knowledge given in the course *Integrated dynamic analysis of wind turbines*, as well as for discussions and help during the master's thesis writing.

I am grateful for the help received from SINTEF. Petter Andreas Berthelsen provided a model and controller basis for use in SIMA, and Marit Kvittem helped with making turbulent wind files. The fast responses and their desire to help is very much appreciated.

I would like to thank the company Dr. Techn. Olav Olsen for providing the master's thesis. In particular, I want to thank the company contact person Håkon S. Andresen for being the link between the company and the Marine Department. In addition, Jonas Gullaksen Straume deserves an extensive thanks for the help, files and discussions about the wind turbine controller calibration and understanding.

At last, I want to thank my fellow students for support and discussion with this thesis. I would also like to thank my family for support and motivation.

Abstract

The objective of this thesis is to evaluate the sensitivity of the tower design with respect to frequencies. The investigation is done for the floating wind turbine concept OO-Star Wind Floater to evaluate if it is possible to reduce the costs of the tower. A comparison of a stiff and flexible tower was done to examine the possibility of introducing a flexible tower to the wind turbine concept. The original concept is made with a stiff tower that resists movement due to loading and has a high first natural frequency to avoid resonance behaviour from the frequencies of the rotating wind turbine.

The sensitivity was first studied with a literature review. In this, challenges for a floating wind turbine and for the tower design was identified. Rules from DNV were evaluated to find tower design and analysis requirements. A model in SIMA was calibrated and a flexible tower and flexible blades were introduced. The investigation was based on time-domain analysis for fatigue and ultimate limit state design.

The tower was made flexible by reducing the elasticity modulus to obtain a desired first tower natural frequency. The method used to reduce the natural frequency is not possible in reality and this gives a limitation on the results. However, the method is considered as reliable for capturing the effects of a flexible tower. The flexible tower was compared to the original stiff tower. The fatigue analysis was used to check for fatigue damage and examine the behaviour of the two models. The ultimate limit state check was done to see if the flexible tower was exposed to material failure due to extreme environmental loads. A spectral analysis investigated resonance behaviour.

The goal was to see if a flexible tower with a lower natural frequency was possible to use on the OO-Star Wind Floater concept, and this proved to be feasible. The tower did not experience fatigue failure during the lifetime. Some excitation in the tower was induced by the rotational frequencies, but it did not lead to fatigue failure. The extreme load cases did not lead to yield or buckling failure, but it is advised to check the yield criteria in further work to ensure a safe design. The check of blade-tip to tower clearance in extreme conditions did not give a satisfactory result with the method used, and further work on this is highly recommended.

The work done in this thesis gives a good indication of a safe design with a flexible tower on the OO-Star Wind Floater. Further work is to make a realistic flexible tower model with first natural frequency in the soft-stiff range. This should be done by varying both the thickness and diameter of the tower.

Sammendrag

Målet med denne masteravhandlingen er å evaluere hvor følsomt tårndesignet til en havvindturbin er med hensyn til rotasjonsfrekvenser fra turbinen. Undersøkelsen er gjort for det flytende havvind konseptet OO-Star Wind Floater for å redusere kostnadene for tårnet. Det er gjort en sammenligning mellom et stivt og et fleksibel tårn for å se om det er mulig å innføre et fleksibelt tårn i konseptet. Det opprinnelige konseptet er laget med et stivt tårn som motstår bevegleser fra vind og bølgelaster. Det stive tårnet har en høy første egenfrekvens for å unngå resonans fra frekvensene til den roterende vindturbinen.

Sensitiviteten til tårnet ble først studert gjennom et litteraturstudie. Da ble utfordringer til en flytende havturbin og til tårndesign identifsert. Regelverk fra DNV-GL ble brukt til å evaluere design og krav til tårnet. Videre ble analyser i tidsdomenet brukt til å analysere utmattelse av tårnet og oppførsel under ekstreme lasttilfeller fra vind og bølgekrefter.

Tårnet ble gjort fleksibelt ved å redusere elastisitetsmodulen til ønsket egenfrekvens. Denne metoden ble brukt for å ha et godt grunnlag for sammenligning mellom den fleksibe og stive modellen, men den fører til at tårndesignet ikke er realistisk og det begrenser bruken av resultatene. Metoden anses imidlertid som pålitelig for å fange effekten av et fleksibelt tårn. Det fleksible tårnet ble sammenlignet med det opprinnelige stive tårnet. Utmattelsesanalysen ble brukt til å kontrollere at tårnet ikke ble utmattet gjennom 25 års levertid og til å undersøke og sammenligne oppførselen til de to modellene. Analysen i ekstreme værtilstander ble gjort for å se om det fleksible tårnet er utsatt for svikt ved høye laster.

Målet var å se om et fleksibelt tårn med lavere egenfrekvens var mulig å bruke på OO-Star Wind Floater-konseptet, og dette viste seg å være gjennomførbart. Tårnet opplevde ikke utmattingssvikt gjennom 25 års livstid. Tårnet fikk noe utslag på eksitasjon fra rotasjonsfrekvensene, men det førte ikke til utmatting og blir derfor ansett trygt. De ekstreme belastningstilfellene førte ikke til knekking eller materialsvikt, men det anbefales at man kontrollerer dette i videre arbeid for å sikre et trygt design. Avstanden mellom turbinens blader og tårnet ble kontrolleret for å forsikre en trygg avstand under høy belastning. Analysen som ble gjort ga ikke et tifredstillende og sikkert resultat, og videre arbeid med dette anbefales.

Arbeidet i denne oppgaven gir en god indikasjon på at det er mulig med et fleksibelt tårn på OO-Star Wind Floater. Videre arbeid er først og fremst å lage et realistisk fleksibelt tårn med første egenfrekvens mellom turbinens rotasjonsfrekvens og blad-passeringsfrekvens. Dette bør gjøres ved å variere både tykkelsen og diameteren av tårnet.

Contents

List of Tables

List of Figures

List of Abbreviations

ALC	Accidental Limit State
BC	Boundary Condition
COG	Centre of Gravity
DFF	Design Fatigue Factor
DLC	Design Load Case
FEA	Finite Element Analysis
FLS	Fatigue Limit State
LCOE	Levelized Cost of Energy
SCF	Stress Concentration Factor
SLS	Serviceability Limit State
ULS	Ultimate Limit State
1P	Rotational Frequency
3P	Blade Passing Frequency
xP	Blade passing frequency for x blades

List of Symbols

ω_n	Circular Frequency
k	Stiffness
m	Mass
ρ	Density
E	Modulus of Elasticity
G	Shear Modulus of Elasticity
f_n	Natural Frequency
f_R	Excitation Frequency
$f_{0,n}$	n^{th} Natural Frequency of the Tower and Foundation
D_c	Cumulative Damage
D_D	Design Damage
$n_{c,i}$	Number of Stress Ranges in Stress Block i
$N_{c,i}$	Number of Cycles to Failure at Stress Range of Stress Block i
T_n	Natural Period
λ_m	Material factor
λ_f	Load factor
$\sigma_{Hotspot}$	Hot Spot Stress
$\sigma_{Nominal}$	Nominal stres
$\sigma_{vonMises}$	von Mises Stress
V_{ref}	Reference Wind Speed
V_{ave}	Average wind speed
I	Turbulence Intensity
H_s	Significant Wave Height
T_p	Spectral Peak Period

Chapter 1

Introduction

This report is the result of the work done for a master thesis in marine structures at the Department of Marine Technology at NTNU. The work is done in collaboration with the company Dr. Techn. Olav Olsen, and will do research on their design of the floating wind turbine concept OO-Star Wind Floater.

1.1 Background

Wind energy is a renewable energy source in which considerable effort is devoted to improving the current industry. The goal is to improve the technology to be more efficient and less expensive so that it can compete with established electricity prices. On-shore wind turbines are limited by the landscape, wind variations and the impact they present on the established infrastructure. The infrastructure will also impose a limit on the size of the wind turbines. Offshore wind turbines experience more stable wind conditions with higher wind speed, which makes them more reliable for power production. Placement of the wind power production unit offshore also has the benefit of less noise pollution and more available space for both larger wind farms and bigger turbines.

In comparison to the oil industry where one structure is needed for obtaining a large amount of fossil fuel, the wind industry needs to consider every opportunity for savings to lower the electricity price. A wind turbine will mainly have costs related to manufacturing, installation and maintenance. A large part of the costs for an offshore turbine is from installation and the number of installed units. This is due to the time-consuming job of installing a high number of individual units and the costs of having ships for transportation and installation. Thus, the industry is moving towards larger turbines with increasing

power rating to reduce the number of installed units for the same total energy output (Duan, 2017).

Challenges with offshore wind turbines are seabed characteristics and water depth. Bottom founded wind turbines are limited to certain soil types and shallow waters. Research is thus done on floating wind turbines to find efficient solutions which can be installed in moderate to deep water and more varied sea bottom properties. The research project Lifes50+ has focused on up-scaling floating wind turbine design concepts for a 10MW turbine. The company Dr. Techn. Olav Olsen was a part of this project with their concept OO-Star wind floater.

To achieve a cost-effective result, every part of the wind turbine is explored to find the best solution. In the project Lifes50+, the tower design was pointed out as one of the components of the structure that was possible to be optimized with regards to costs (Tecnalia, 2017). The wind turbine tower for a floating concept is subjected to significant fatigue and thus often designed as a stiff structure. To lower the costs of the tower, the amount of material used should be reduced. This leads to a more flexible tower with a lower eigenfrequency. A lower eigenfrequency is in danger of coinciding with the wind turbine rotational frequencies, which can lead to significant response and danger of fatigue failure. There is also a possibility that a more flexible tower will be more sensitive to extreme load cases.

1.2 Problem Formulation

This thesis will examine if the tower design can be optimized to reduce costs for a high MW turbine. The goal of a tower design can be formulated as "to achieve the desired tower height with the required stiffness at the lowest possible construction costs" (Hau, 2013). In order of achieving a more cost-effective tower, the tower must be made more flexible.

The main objective of this thesis is to evaluate the sensitivity of the tower design for the offshore wind turbine concept OO-Star Wind Floater with respect to the rotational frequencies of the turbine. The specific components that are addressed are:

1. Literature review of principles for analysis and design, and challenges related to a floating wind turbine.
2. Identify challenges of a flexible tower and find possible ways of reducing the tower natural frequency.

3. Calibration of an existing potential theory model of the floater. Include a flexible tower and blades for analysis.
4. Perform coupled, stochastic time-domain analysis for long term fatigue evaluation.
5. Vary the stiffness of the tower and perform fatigue evaluation. Discuss a priori estimation of its impact on fatigue damage.
6. Use extreme environmental conditions to determine the characteristics of blade tip clearance and utilization with regards to buckling and yielding of the tower.

1.3 Limitations

The results of the thesis are limited by the approach chosen for reduction of the first tower natural frequency. The reduction is done by reducing the elasticity modulus to a level not realistic. This is a good strategy for checking the behaviour of a flexible tower and to compare it to the original stiff tower, but the results do not give a functional tower design. This also limits the calculations for yielding and buckling since the material properties not correct.

The fatigue analysis is limited by the number of load cases and wave seeds chosen. The limitation leads to a result which perhaps does not capture the entire lifetime in its representation, but the trend is possible to see. The buckling check is only done with formulas, and a buckling check in a proper software could be needed to verify the results. The check of the distance between the blade-tip and tower is very limited by the output from the analysis which made it difficult to ensure a proper distance during extreme loading.

1.4 Approach

A literature study is conducted to examine the background of tower design and to shed light on challenges in the design of a floating wind turbine. Design standards and rules are studied to find requirements for the tower design. The model provided in SIMA is tested and calibrated against results found in the literature. A flexible tower is found by reducing the elasticity modulus of the material. The controller is adjusted due to the changed tower frequency.

A fatigue damage assessment is executed in SIMA for both the current tower and the adjusted tower for comparison. This is done for a selected set of representative environmental states. The ultimate limit state is also examined briefly in SIMA for extreme environmental states, and the blade tip clearance to the tower is found to check if the distance is safe and within regulations. Both a check of yielding and buckling is done according to DNV calculations.

Chapter 2

Literature review

This chapter provides a brief review of the literature that exists on the topics stated in the problem formulation. It starts with a review of analysis and design for an offshore wind turbine according to the standards provided by DNV-GL. Then it identifies challenges with a floating wind turbine compared to a fixed wind turbine structure.

After a brief assessment of the principles for wind turbine design, the chapter continues with a more detailed survey of the wind turbine tower. The tower natural frequency is studied and possible challenges are examined.

2.1 Principles for Design and Analysis of Offshore Wind Turbines

An offshore wind turbine design should be based on first principles to ensure an innovative design that improves the effectiveness or reduce the costs (Bachynski, 2018). First principles in sciences can be defined as "if it starts directly at the level of established science and does not make assumptions such as empirical model and parameter fitting" (Wikipedia, 2019).

The design process of an offshore wind turbine concept is based on a design spiral with a continuous iteration loop. The iteration starts with finding a feasible design, and later approach an optimal solution. The state-of-the-art design process consists of three stages, and the stages are usually overlapping because new information is found during the design loop. The stages are briefly described in figure 2.1. In addition, also risks, safety, functionality, levelized cost of energy and manufacturing & deployment must be considered in the design process to achieve a feasible and optimal design.

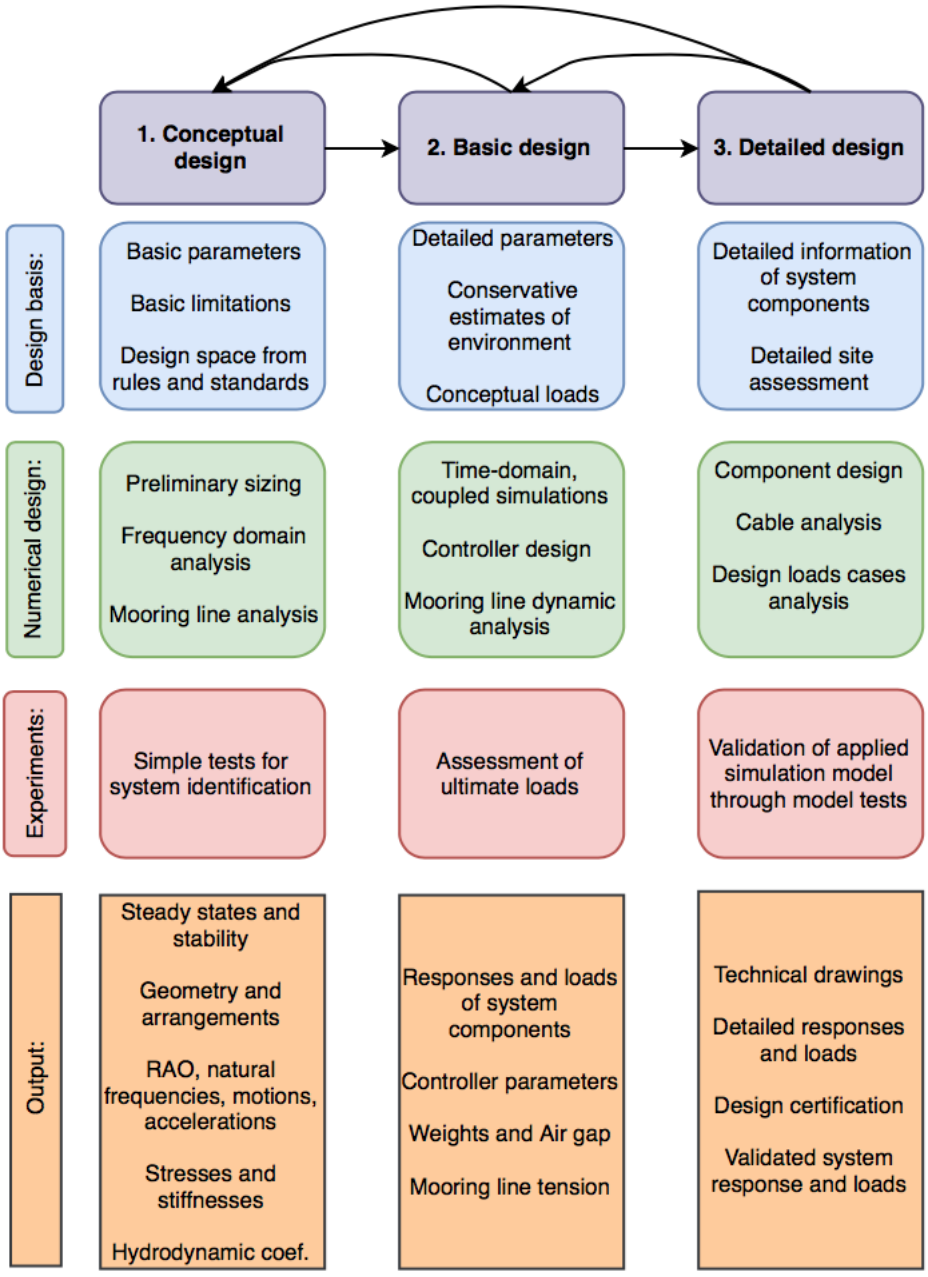

Figure 2.1: State-of-the-art design process inspired by (USTUTT, 2016)

.

According to DNV-OS-J101 (DNV, 2014), the structural design must be made with a certain safety class based on failure consequences. For offshore wind turbines, a *Normal Safety Class* is considered sufficient since the structure is normally unmanned during severe environmental conditions. The safety class is reflected in the requirements of the load factors to ensure a safe design. The target safety level for a normal safety class is a nominal annual probability of failure of 10^{-4}.

The design procedure in DNV-OS-J101 for offshore wind turbines is based on the partial safety factor method. This is a design method which ensures that the target safety level is obtained by applying safety factors to characteristic values of the governing variables. The safety factors are divided into material, resistance and load factors. The requirements for the factors are based on ensuring an unfavourable realization of the responses so that a satisfactory safety level is achieved. The material factor is independent on the safety level that is chosen, while the load and resistance factors are used to control the safety level.

The design of an offshore wind turbine is based design against limit states. A limit state is "a condition beyond which a structure or structural component will no longer satisfy the design requirements" (DNV, 2010). DNV standards consider the four limit states:

- Ultimate limit state (ULS): maximum load-carrying resistance
- Fatigue limit state (FLS): failure due to cyclic loading
- Accidental limit state (ALS): maximum load-carrying resistance for accidental loads or integrity for damaged structures
- Serviceability limit state (SLS): tolerance criteria for normal use

In addition to the limit states, DNV-OS-J103 also has a requirement for the floater motion control to minimize excitation of floater motions. This is a specific demand for floating wind turbines and will be discussed further in section 2.2.

Figure 2.2 gives the load factors for ULS and ALS. For fatigue limit state, the requirement is that the structure shall resist the expected fatigue loads applied from all different phases of the structure's lifetime. Thus, the FLS load factor is $\gamma_f = 1$. The material factor is 1 for ALS and SLS. For FLS, the material factor is not used because fatigue assessment is based on an overall Design Fatigue Factor (DFF). Material factors in ULS depend on the component studied.

Table 5-1 Load factors γ_f for the ULS and the ALS

Load factor set	*Limit state*	*Load categories*					
		G	*Q*	*E*			*D*
				Safety class			
				Low	*Normal*	*High*	
(a)	ULS	1.25	1.25	0.7 (*)			1.0
(b)	ULS	1.0	1.0	1.20	1.35	1.55	1.0
(c)	ULS for abnormal wind load cases	1.0	1.0	1.1			1.0
(d)	ALS	1.0	1.0	0.9	1.0	1.15	1.0

Load categories are:
G = permanent load
Q = variable functional load, normally relevant only for design against ship impacts and for local design of platforms
E = environmental load
D = deformation load.
For description of load categories, see Sec.4.
(*) When environmental loads are to be combined with functional loads from ship impacts, the environmental load factor shall be increased from 0.7 to 1.0 to reflect that ship impacts are correlated with the wave conditions.

Figure 2.2: Partial safety factors for loads (DNV, 2010).

.

Design load cases (DLC) are used to verify the structural integrity of the wind turbine concepts. The load cases are combinations of loads acting on the structure for each situation applicable. DNV states a minimum of design load cases and requires that the designer always considers if other cases can lead to more severe loading. The load cases state the appropriate analysis for the limit states. Figure 2.3 gives some of the DLCs required by DNV for certification. The DLCs cover loads from all phases an offshore wind turbine is subjected to, as power production, faults, startup, shutdown, emergency, parked turbine and combinations of these. In addition, the transportation, assembly. maintenance and repair are included in the design load cases recommended.

Design Situation	DLC	Wind Condition	Marine Condition				Other Conditions:	Type of Analysis		Partial safety factor
			Waves	Wind and wave directionality	Sea Currents	Water Level		Onshore	Offshore	
1) Power Production:	1.1	NTM $V_{in} < V_{hub} < V_{out}$	NSS $H_s = E[H_s \mid V_{hub}]$	COD, UNI	NCM	MSL	For extrapolation of extreme loads (offshore – only RNA)	U	U	N (1.25)
	1.2	NTM $V_{in} < V_{hub} < V_{out}$	NSS Joint prob. distribution of H_s, T_p, V_{hub}	MIS, MUL	No Currents	NWLR or ≥ MSL		F/U	F/U	F/N
	1.3	ETM $V_{in} < V_{hub} < V_{out}$	NSS $H_s = E[H_s \mid V_{hub}]$	COD, UNI	NCM	MSL		U	U	N
	1.4	ECD $V_{hub} = V_r - 2$ m/s, V_r, $V_r + 2$ m/s	NSS $H_s = E[H_s \mid V_{hub}]$	MIS, wind direction change	NCM	MSL		U	U	N
	1.5	EWS $V_{in} < V_{hub} < V_{out}$	NSS $H_s = E[H_s \mid V_{hub}]$	COD, UNI	NCM	MSL		U	U	N
	1.6	NTM $V_{in} < V_{hub} < V_{out}$	SSS $H_s = H_{s,SSS}$	COD, UNI	NCM	NWLR		-	U	N
	1.7	NTM $V_{in} < V_{hub} < V_{out}$	NSS Joint prob. distribution of H_s, T_p, V_{hub}	MIS, MUL	No Currents	NWLR or ≥ MSL	Ice formation	F/U	F/U	F/N
2) Power Production + occurrence of fault:	2.1	NTM $V_{in} < V_{hub} < V_{out}$	NSS $H_s = E[H_s \mid V_{hub}]$	COD, UNI	NCM	MSL	Normal control system fault or primary layer control function fault	U	U	N
	2.2	NTM $V_{in} < V_{hub} < V_{out}$	NSS $H_s = E[H_s \mid V_{hub}]$	COD, UNI	NCM	MSL	Abnormal control system fault or secondary layer protection function fault	U	U	A
	2.3	EOG $V_{hub} = V_r \pm 2$ m/s and V_{out}	NSS $H_s = E[H_s \mid V_{hub}]$	COD, UNI	NCM	MSL	External or internal electrical fault including loss of electrical network	U	U	A
	2.3 alternatively	NTM $V_{in} < V_{hub} < V_{out}$	NSS $H_s = E[H_s \mid V_{hub}]$	COD, UNI	NCM	MSL	External or internal electrical fault including loss of electrical network	U	U	N
	2.4	NTM $V_{in} < V_{hub} < V_{out}$	NSS $H_s = E[H_s \mid V_{hub}]$	COD, UNI	No currents	NWLR or ≥ MSL	Normal control system fault or loss of electrical network or primary layer control function fault	F/U	F/U	F/N
	2.5	NWP $V_{in} < V_{hub} < V_{out}$	NSS $H_s = E[H_s \mid V_{hub}]$	COD, UNI	NCM	MSL	Fault ride through	U	U	N (1.20)

Figure 2.3: Design load cases from (DNV, 2016b)

.

Fatigue limit state is considered to be the constraining limit state for the design of a wind turbine tower and will thus be discussed in section 3.5. In ultimate limit state assessment, it is important to check the capacity of all structural components for both yielding and buckling. The accidental limit state is done by checking the remaining capacity after an accidental load has occurred. Serviceability limit state includes deflections and vibrations which influence operations. The accidental and serviceability limit states will not be assessed in this thesis because they are not considered to be decisive for the design of the turbine tower.

DNV-OS-J103 for floating offshore wind turbines requires that the load cases are calculated through coupled analysis. The result must also be verified with model tests or other well-known and tested simulation programs. A coupled analysis "means that the structural dynamic responses from the aerodynamics and hydrodynamics loads are coupled" (DNV, 2010). It is common to perform a time-domain analysis for floating wind turbines to capture the effect of variation in loading from the surrounding environment. The simulation length for the analysis depends on the type of load case. For normal production cases,

the simulation lengths can be described to:

- ULS analysis: Simulation length should be at least 3 hours.
- FLS analysis: Simulation length can be 1 hour or less.

According to DNV standard DNV-OS-J101, at least 3 seeds per wind speed should be used. Different seeds for the same wind climate give different load effect realizations. Wave seeds contain information on the "start position of the waves, the wavelength and amplitude, and the lifetime by specifying when the waves are born and fading out" (Dong-young Kim et al., 2011). They give the information needed to present the wave climate.

The design life of an offshore wind turbine is the time period over which the structure is designed to maintain the required level of safety. Within this scope, inspection and maintenance are required to lower the necessary strength to survive the entire design lifetime. The design lifetime is usually 20-25 years for an offshore wind turbine.

2.1.1 Integrated Dynamic Analysis of Floating Wind Turbines

The dynamics associated with a floating wind turbine is illustrated in figure 2.4. It is seen that the floating wind turbine will experience several environmental conditions simultaneously which all contribute to dynamic loads and responses. Because of this, the analysis of a floating wind turbine should include all load sources at the same time to ensure correct analysis of the couplings between the load sources and the corresponding behaviour of the structure. In principle, it is aerodynamic loads due to the air moving around the structure and hydrodynamic loads from waves and currents that are the most important environmental factors. In addition, effects of tide and storm surge, soil, icing and lightning can be included to look at special cases in the lifetime of the turbine (Bachynski, 2018).

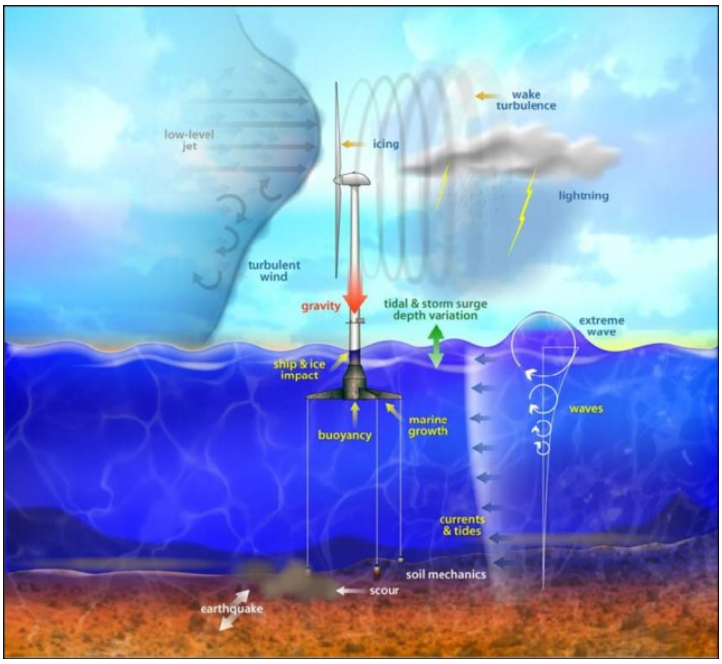

Figure 2.4: Dynamics associated with floating wind turbine (Sirnivas et al., 2014)

An integrated dynamic analysis is necessary to be able to predict the dynamic behaviour of a floating wind turbine. The analysis should include a load analysis, response analysis and controller theory to find the real response of the floating wind turbine. The analysis is done in the time-domain because both the loads and the responses develop with time over multiple frequencies. A frequency response analysis is also useful to check which frequencies are excited and thus find the dynamic performance (Bachynski, 2018).

A floating wind turbine experience aero-hydro-servo-elastic coupling, which "implies a coupling between the aerodynamic loads and responses, the hydrodynamic loads and responses, the control system and the deformation response of the structure due to elasticity" (DNV, 2010). Usually, in an analysis, the environmental conditions are not modelled with coupling, so the wind and waves are independent of each other in the simulations. In an integrated coupled dynamic analysis, all force and response equations are solved simultaneously at each time step to ensure correct responses (DNV, 2010).

2.2 Challenges and Advantages of a Floating Wind Turbine

The main challenge for a floating wind turbine compared to a bottom-fixed is the wave response and the motions of the platform (Jiang et al., 2018). More active dynamics result in higher tower top motions and a coupling between the rotor and the support structure (Butterfield et al., 2007).

A floating wind turbine has a floating platform and needs a station-keeping system. This increase the complexity of the system and an advanced numerical tool is necessary to capture the dynamic behaviour (Jiang et al., 2018). The structure must ensure sufficient buoyancy and stability to support the weight of the wind turbine and the mooring lines must limit the motions within acceptable limits (Butterfield et al., 2007).

The station-keeping system consists of different types of mooring depending on the type of floating platform. There are three main types of floating platforms for offshore wind turbines. A spar platform mainly uses ballast to stabilize, a semi-submersible its buoyancy and a TLP utilizes the mooring lines (Bachynski, 2018). The types are shown in figure 2.5. The mooring system of a TLP has vertical mooring lines which does not take up much area, but the anchors are sensitive to the type of seabed. The other two types have a catenary mooring system, and this takes up the area around the structure but the anchors are less sensitive to the seabed properties. Also, the water depth influences the choice of mooring system that is cost effective. A catenary mooring system can be used in shallower water, but in very deep water it will not be a cost-effective solution because of very long lines necessary. A TLP cannot be used in shallow water (Butterfield et al., 2007).

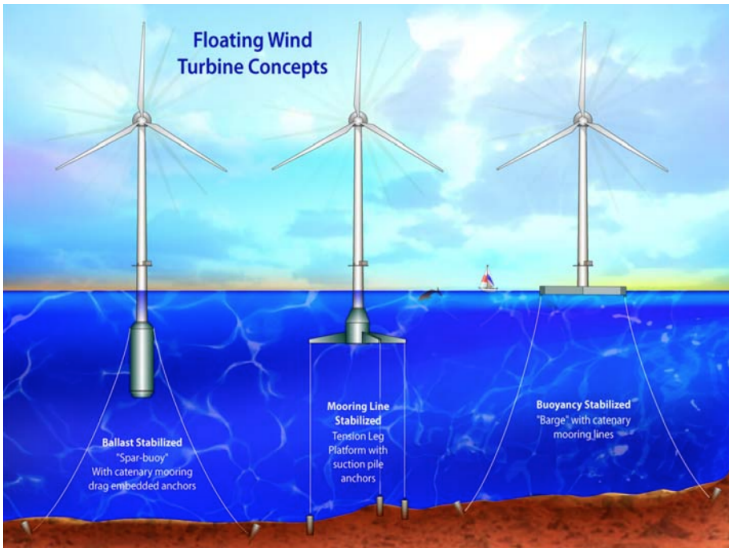

Figure 2.5: Typical Floating Platform Static Stability Concepts (Butterfield et al., 2007)

A motion control system is used for wind turbines to control the performances and operations. For floating wind turbines, the control system can be used to limit the response of the combined turbine and platform system, and to reduce the wave loading. Operational control is used to influence the blade pitch, yaw motion of nacelle and generator torque. It is also necessary to have a supervisory control to switch between operational states of the turbine (Bachynski, 2018). The complexity of the control system increases when the wind turbine has a floating substructure. The floating control system is used to reduce undesired motions (Butterfield et al., 2007). This is discussed further in section 3.2.5.

The control system is also used to avoid the problem of negative damping. This is only an issue for floating wind turbines. The problem occurs when the floating turbine leans forward in the wind direction. This is problematic because it reduces the thrust which will impose negative damping in surge and pitch motions of the structure. Negative damping may lead to a large amplification of the motion and responses. It is therefore important to design a control system specifically for a floating wind turbine to avoid the situation with negative damping. This is done by allowing the control system to adjust the blades such that the thrust is constant with the motions of the platform.

The advantages of a floating wind turbine depending on the type of platform chosen. All types of platforms can be made stable for transportation from the yard to the site. This makes it possible to assemble the entire structure in a calm sea state without expensive installation vessels. When the structure is towed to site, the towing and installation can be done in a broad range of weather conditions. Towing to the site is most applicable for a spar platform, but the other types can be designed to also manage this operation. A stable semi-submersible with low draft can be towed into port for long-term maintenance, which can lower the maintenance costs and reduce the weather condition limitation. The decommissioning of a floating platform is a less complicated procedure compared to a bottom-fixed wind turbine, which also can reduce the costs of this part of the life cycle (Butterfield et al., 2007).

2.3 Aspects and Challenges of a Wind Turbine Tower Design

The tower of a wind turbine is defined as a "structural component, which forms a part of the support structure for a wind turbine, usually extending from somewhere above the still water level to just below the nacelle of the wind turbine" (DNV, 2014). This section will review the tower design and requirements for a safe design. Furthermore, the allowable change of the tower stiffness and measures to change it will be discussed.

Wind turbine towers are usually a cylindrical tapered structure with a larger base diameter than the top diameter. Important aspects are stiffness, mass reduction, tower shadow and blade tip clearance. Stiffness and mass reduction are related to safe and cost-effective design. Tower shadow is an effect on the thrust force which gives a variation in the thrust every time a blade passes the tower since the tower will influence the inflow (Bachynski, 2018). Blade tip clearance is investigated in section 2.4, and ensures that the blade and tower avoid collisions.

Tubular steel towers are most common for offshore wind turbines. An alternative to using steel for the towers is to introduce concrete. It is possible to make the tower completely in concrete or to have a hybrid solution (Hau, 2013). The material choice is dependent on fabrication, installation, costs and weight. Fabrication can limit the dimensions and can be costly for complex methods. Installation depends on transportation length, dimensions of the structure, costs and available cranes for lifting operations.

"The proportioning of wind towers is typically controlled by a combination of ultimate bending strength, fatigue and resonance avoidance" (Jay et al., 2016). A larger wind turbine needs a taller tower. It is expected that taller towers have a high slenderness ratio to ensure an optimal stiffness to weight relationship. The slenderness describes the ratio D/t or diameter-to-thickness. Conventional towers have a slenderness ratio of about 300, while taller towers can have ratios up to 500. High slenderness ratios for a cross-section make the structure very sensitive to imperfections, for example in welds. This means that the tower can become exposed to buckling failure under ultimate bending loading. There is limited experience on towers with high slenderness, and great care must be taken to ensure a good balance between weight reduction and ultimate failure (Jay et al., 2016).

2.3.1 Natural Frequency Considerations for the Tower

This subsection evaluates the behaviour of the first natural frequency of the tower and which regions it is allowed to be within. All structures have several natural frequencies which are the frequency the structure will start to vibrate with if it is exposed to a certain external dynamic load. If the force applied to the structure has the same frequency as its natural frequency, the structure will experience resonance and a small load will give large vibrations. Vibrations lead to fatigue failure and must be limited to ensure a safe design during the lifetime. The natural frequencies depend on the mass and stiffness of the structure and how these are distributed (Community, 2018). The circular frequency for a simple undamped spring-mass system is given in equation 2.1. This shows that the relationship for the natural frequency is dependent on the stiffness k over the mass m.

$$\omega_n = \sqrt{\frac{k}{m}} \tag{2.1}$$

Offshore wind turbine structures are dynamically loaded by a combination of hydrodynamic and aerodynamic forces. The hydrodynamic forces are from waves and currents, while the aerodynamic forces have origin in the rotor and wind loading. The dynamic loads that should be assessed for the natural frequency of the structure are: (Arany et al., 2016):

- Wind turbulence
- Waves
- Rotational frequency from blades (1P)
- Blade passing frequency (3P)
- Mechanical components and control system

Figure 2.6 gives a description of normal dynamic loads on an offshore wind turbine. The wind turbulence and wave loads are described with power spectral densities at offshore locations (Arany et al., 2016). In this figure, it can be seen that the wind and wave frequencies are below or coinciding with the rotational frequency from the blades (1P). Then there is a gap between the rotational frequency and the blade passing frequency. The blade passing frequency depends on the number of blades, and for a three-bladed turbine, it is 3 times P, where P represents the rotational frequency. Figure 2.6 also shows a trend that larger turbines with more rated power tend to have lower values on the frequency regions for the aerodynamic forces.

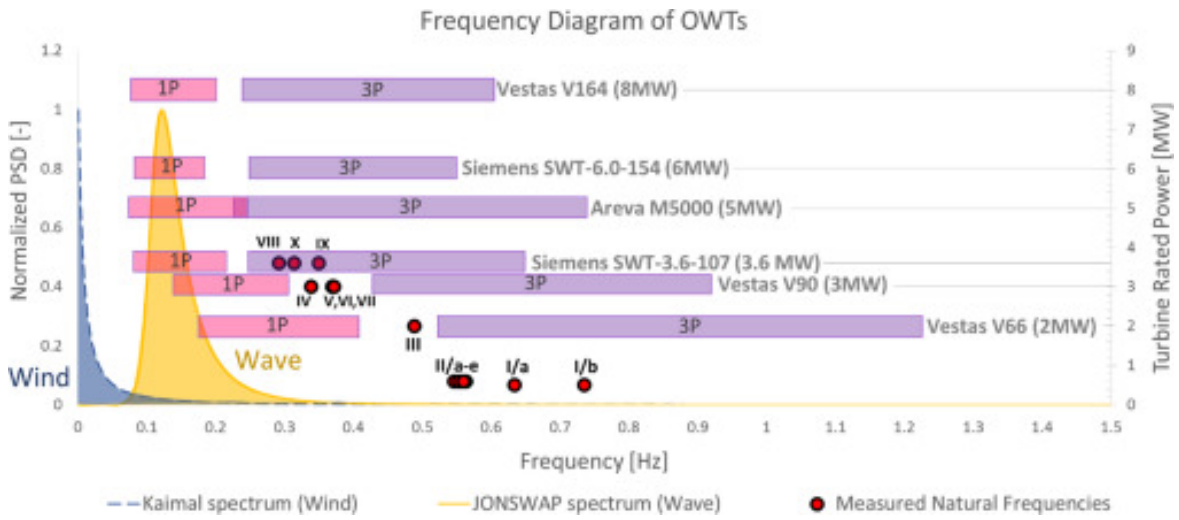

Figure 2.6: Typical rotational frequencies (1P) and blade passing frequency (3P) for different sized turbines and in relation to some wind and wave spectra and the measured natural frequency (Arany et al., 2016)

.

The rotational frequency (1P) of the rotor is due to a "load caused by the vibration at the hub level because of the mass and aerodynamic imbalances of the rotor" (Bhattacharya, 2014). The wind turbines have variable speeds it can operate with, so the aerodynamic frequencies are ranges between the lowest and highest revolution per minute (rpm). The blade passing frequency is due to shadowing effects of the blades on the tower. When a blade is in front of the tower, it will produce a loss of wind load on the tower. Since this is obtained by taking the limit of rotational frequency times the number of blades, this is also over a frequency range (Bhattacharya, 2014). The wind and wave frequencies can be found from statistics and should be found for each site the wind turbine is considered for.

Figure 2.7 gives the tower stiffness categories used when designing the tower of a wind turbine. These give the relationship between the first natural frequency of the tower and the exciting frequencies from the rotor thrust fluctuations (Burton, 2011). A stiff-stiff tower has its natural frequency above both 1P and 3P frequencies. This gives a very simple and safe design because the tower is not excited by the rotor. In this design, the tower natural frequencies are not encountered during start-up or shut-down of the turbine (Hau, 2013). In addition, a stiff design tends to radiate less sound than a flexible tower (Miceli, 2017). However, a stiff-stiff design requires a large mass and thus it presents a high cost.

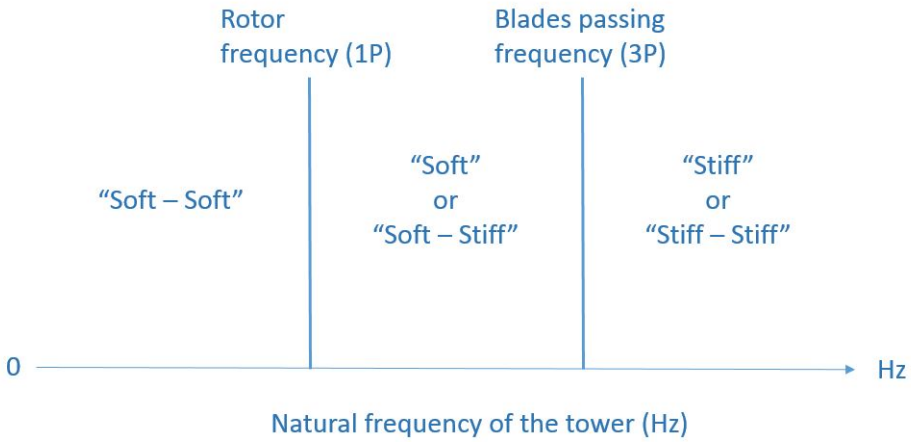

Figure 2.7: Description of tower stiffness categories (Miceli, 2017)

.

A soft-stiff design is in between the 1P and 3P regions of frequency. This is normal for bottom fixed offshore wind turbines since it is not very close to the wave frequency or wind frequency and the more flexible design is cheaper. Because of the environmental frequencies, a soft-soft design for an offshore wind turbine is uncommon. A soft-stiff design of the tower will require a more detailed dynamic analysis to ensure a safe design. A flexible tower design leads to a cost-effective design if made with an acceptable safety class.

All vibrating or moving components on the wind turbine can lead to resonance if there is a strong coupling between the tower and the component. A floating wind turbine is a complex system because it has a lot of couplings and experiences several different external and internal vibrations. Thus, it is normally impossible to avoid all resonances (Luan, 2018). Important aspects when designing the tower is thus to ensure that it has the ability to withstand resonances and their respective loads at normal conditions for the turbine. Not avoidable resonances should occur at conditions the turbine has limited time in to ensure low damage (Huhn, 2015).

2.3.2 Natural Frequency Requirements

DNVGL-ST-0126 (DNV, 2016a) gives a safety criterion for the avoidance of excitation frequencies from the rotational frequencies of the rotor. This is given in equation 2.2. Here, f_R is the excitation frequency for the rotating frequency range for 1P and 3P. $f_{0,n}$ is the n^{th} natural frequency of the tower and foundation

for the complete system. This criterion gives a 5% margin to account for uncertainties in the calculation of natural frequencies.

$$1.05 \leq \frac{f_R}{f_{0,n}} \leq 0.95 \tag{2.2}$$

2.3.3 Natural Frequency Allowance for a Soft-Stiff Tower

Table 2.1 gives the 1P and 3P range for the DTU 10MW reference turbine. The tower natural frequency should be between these to have a soft-stiff tower design. Based on this and the requirement in equation 2.2, it is possible to find an allowed range for the first natural frequency of a soft-stiff tower. Figure 2.8 gives the allowed frequency window based on wind, waves and rotor frequencies. As displayed in figure 2.6, the wind spectrum has its power spectral density well below the 1P range. The wave spectrum for an undeveloped sea state with a JONSWAP spectrum has its peak around 0.15 Hz and low content above 0.2 Hz. A developed sea state with a Pierson-Moskowitz spectrum has its power spectral density spectrum shifted towards lower frequencies than the JONSWAP spectrum in figure 2.6 (Haritos, 2019), so a limit of 0.2 Hz is set to the minimum tower frequency to reduce dynamic excitation from the waves. A "natural frequency closer to the excitation frequency of the wave and wind makes the structure more sensitive to dynamics" (Arany et al., 2016). It is thus important to check the dynamic responses of a soft-stiff wind turbine with a high MW rating. The resulting range for the first natural frequency of a soft-stiff tower becomes 0.2-0.28 Hz.

Property	**Value**
1P range	0.1-0.16 Hz
3P range	0.3-0.48 Hz

Table 2.1: 1P and 3P range for the DTU 10 MW reference turbine (Christian Bak, 2013b) (Xue, 2016)

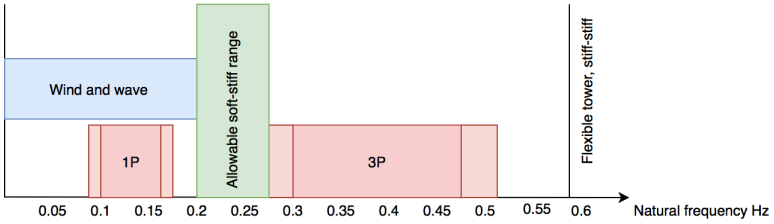

Figure 2.8: Allowed range for a soft-stiff tower

.

2.3.4 Measures to Change the Natural Frequency of the Tower

The natural frequency of the tower is mainly dependent on mass, stiffness, geometry and material properties. Tuning of it can thus be done with different methods and some of them will be discussed for a floating wind turbine tower.

The simplest way of influencing the natural frequency of the tower is to change the base diameter. The frequency increases with diameter. Thus, a way of ensuring a soft-stiff tower could be to decrease the base diameter. The natural frequency of the tower depends on the stiffness over mass and distribution of these. For a lower natural frequency, it would be best to decrease the stiffness instead of increasing the mass since a higher mass would influence costs and installation. It is important to verify that the strength against extreme loads and fatigue loads is sufficient when decreasing the dimensions (Burton, 2011). It is also possible to change the wall thickness and have varying thickness with the stages in diameter. It would then be possible to have a higher thickness at the base where the bending moment is largest and a thinner structure at the tower top (Hau, 2013).

Another way of tuning the natural frequency is to change the material. For the OO-Star wind Floater, it is also possible to change the interface between the concrete shaft and steel tower. Concrete is not sensitive to fatigue compared to steel, so it is a good alternative material to use. Increasing the concrete shaft and having a lower steel tower height can change the tower natural frequency since the dimensions must be changed for the new design.

2.4 Challenges with Blade-Tip Clearance

Most offshore wind turbines have an upwind configuration of the blades so that the wind first meet the blades before it passes the tower. This configuration has the advantage of less tower shadow effect which reduces the dynamic load on the blade and noise effects. Tower shadow is a term describing that the wind speed is influenced by the tower. An upwind blade configuration can lead to blade-tower collisions in extreme situations where the flexible blades are near the tower. Great care must be taken to avoid the risk of strikes between the structural components. This "requires accurate prediction of blade deflections under turbulent wind loading" Burton (2011).

Measures are taken to ensure an acceptable blade-tower clearance is to tilt the low-speed shaft upwards or increasing the rotor overhang. If the low-speed shaft is tilted upwards, the blades will have a larger clearance when passing in front of the tower. The tilting is often between 5° and 6°. The consequence of the tilting is a very small reduction in power output. The other option, increasing the rotor overhang, is less used because it will increase the size of the low-speed shaft and increase the nacelle bedplate bending moments (Burton, 2011). The rotor overhang is the "distance from the axis of the wind turbine tower to the centre of the hub" (Bhattacharya et al., 2014). Figure 2.9 gives an illustration of how the shaft is tilted and that the flexible blades have a prebend angle away from the tower.

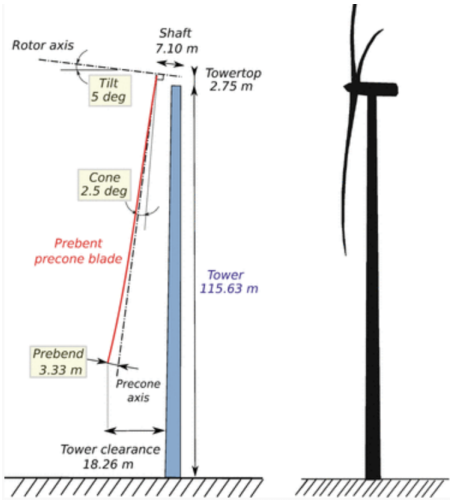

Figure 2.9: Illustration of tilt, blade bending and tower clearance form Horcas et al. (2016)

.

The blade tip clearance to the tower depends on the flexibility of the blade and motions of both structural components compared to each other. The blade tip deflection should be found and seen in comparison

with how the tower moves relative to the blades for a floating wind turbine. If the tower is made more flexible, an assessment of how both the blades and tower deflects and rotates is necessary to ensure that there is no danger of interaction.

Chapter 3

Methodology

This chapter describes the methods used and discusses their applicability. First, the software is described to give a reference for further use of it. Then the model used of the OO-Star Wind Floater is explained and the adjustments of the tower are described. The model is tested against results from the literature to validate the behaviour. Finally, the types of analysis are explained to the extent that it is possible to reproduce the results. The design load cases and types of analysis are justified. Only fatigue and ultimate limit states are used to check the design in accordance with the objectives. This is because fatigue is considered crucial for the design of towers and ultimate limit state could become important with a more flexible design.

3.1 Software: SIMA

The software used in this thesis is named SIMA, which stands for *simulation workbench for marine applications* and is developed by MARINTEK and Centre for Ships and Ocean Structures (CeSOS) in Trondheim, Norway. A coupled SIMO/RIFLEX model has been provided from SINTEF Ocean for use in the software SIMA. This model is the public version of the OO-Star Wind Floater from the project Lifes50+.

SIMA is a workbench that "offers a complete solution for simulation and analysis of marine operations and floating systems" (SINTEF). It provides a finite element analysis in the time domain and can perform fully coupled or decoupled analysis. In a coupled analysis, the feature RIFLEX is in control and uses the SIMO as input (Bachynski, 2018). SIMO models the hydrodynamic loads on a floating rigid-body in the time-domain based on potential theory. RIFLEX is a finite element solver and models the mooring lines,

tower, shaft and blades. AeroDyn is used to read a turbulent wind field and to calculate the aerodynamic loads based on Blade Element Momentum theory (Li et al., 2017).

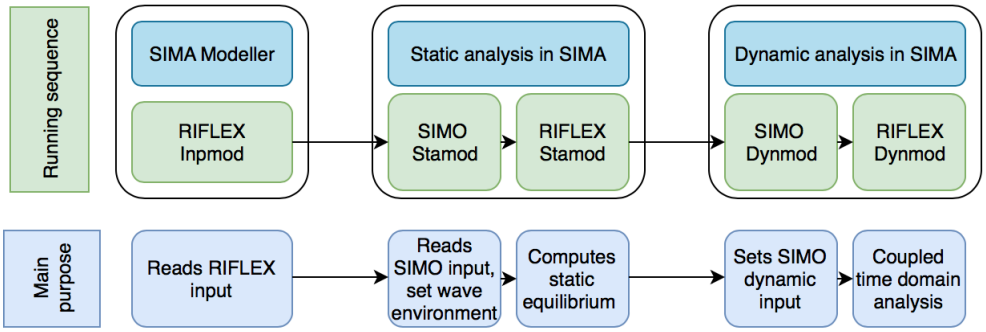

Figure 3.1: Running sequence for a coupled SIMO/RIFLEX model in SIMA, adopted from Bachynski (2018)

Figure 3.1 describes the running sequence and main purpose of a SIMO/RIFLEX model in SIMA. First, the RIFLEX Inpmod reads the input files and check for missing files. Then the static analysis with no wind is established with first the SIMO Stamod which reads the SIMO input and set wave environment. Next, the RIFLEX Stamod computes static equilibrium for the coupled system with no wind forces by using the environmental information from SIMO. The results for the static analysis is used as a starting point for the dynamic analysis. The SIMO dynamic input and wave generation is established in SIMO Dynmod. These are input to the RIFLEX Dynmod which executes a coupled time-domain analysis. After this step, output files can be generated as desired (Bachynski, 2018).

Since the static calculation does not include the wind environment, the turbine performance can only be found from a time domain analysis. The turbine will always start from a standstill condition. The consequence of this is that a long simulation length is required for the turbine to reach a steady-state condition. The transient phase with the startup time of the simulation must be removed from the response output.

The tower and blades are modelled with nonlinear beam elements which can account for large deflections (Li et al., 2017). The semi-submersible is made of slender elements describing the behaviour and properties of the components. The controller is user-defined and has its basis from the DTU 10 MW controller, but it is calibrated for the platform and tower used. The mooring lines are modelled with bar elements.

3.2 Model Description of the OO-Star Wind Floater

The model of the OO-Star Wind floater was provided by SINTEF Ocean and is the public model used in the project Lifes50+. The design is developed and patented by Dr. Techn. Olav Olsen. The model is a coupled SIMO-RIFLEX model to use in the software SIMA. The model is used with the DTU controller and flexible blades are included with help from supervisor Stian Sørum.

This section will describe the design of the OO-Star Wind Floater. Results from Lifes50+ and other relevant sources will be used to evaluate the performance of the model. This section will also describe how the tower is changed to have a soft-stiff first natural frequency.

3.2.1 OO-Star Wind Floater

The OO-Star Wind Floater is a 3-leg semi-submersible with a central shaft supporting the wind turbine. It has a passive ballast system and permanent buoyancy in the columns and shaft. The floating structure has a three star-shaped pontoon with three buoyancy cylinders. The columns provide stability, and the pontoon gives structural support to the columns in addition to weight stability, damping and added mass (Landbø, 2018).

The structure can be fabricated in a dock. It is made feasible for modular fabrication and can be fully assembled at quay-side with low water depth. After assembly, the entire structure with wind turbine can be towed to the site. This means that there is no need for expensive heavy offshore lifts (Landbø, 2018).

The floating platform is made of concrete. Concrete is a good choice because it is not fatigue sensitive and thus have a long design life of more than 100 years. This makes it possible to reuse the floater with new wind turbines. The tower is made of steel while the shaft that connects the semi-submersible and the tower is in concrete. This makes the structure a hybrid type tower. The company Dr. Techn. Olav Olsen has pointed out a possibility of "improving cost and durability by lifting the interface between concrete and steel to reduce steel tower fatigue" (Landbø, 2018). Figure 3.2 displays the model design.

Figure 3.2: OO-Star Wind Floater (Landbø, 2018)

3.2.2 Wind Turbine

The turbine used in the model is the DTU 10MW Reference Wind Turbine from the project Lifes50+. Table 3.1 gives the main parameters that are relevant in this thesis (DTU, 2015).

Parameter	Description
Rotor orientation	Clockwise rotation - upwind
Control	Variable speed Collective pitch
Cut in wind speed	4 m/s
Cut out wind speed	25 m/s
Rated wind speed	11.4 m/s
Rated power	10 MW
Number of blades	3
Rotor diameter	178.3 m
Rotor speed	6-9.6 rpm
Shaft tilt angle	5°
Blade prebend	3.332 m
Rotor precone angle	-2.5°

Table 3.1: Turbine parameters of the DTU 10MW Reference Wind Turbine, adopted from DTU (2015)

The model provided in SIMA was equipped with stiff blades with a constant and high stiffness along the length. In reality, the blades will have decreasing stiffness along the length from the root. Flexible blades were decided to be included in the model because the blade flexibility will influence the eigenmodes of the model. The correct eigenmodes are important in this thesis to find the correct tower frequency and evaluate resonant behaviour. By comparison of the eigenmodes with stiff and flexible blades, it was clear that only the flexible blades lead to eigenmodes involving the blades. Flexible blades will also influence the blade-tip to tower clearance discussed in section 2.4. The model was adjusted with flexible blades provided by supervisor Stian Sørum which has the properties of the DTU 10MW reference turbine defined by Christian Bak (2013a). The blade model differs slightly from the original because "the inner airfoils are modified to avoid anomalous lift coefficients" (Erin E. Bachynski, 2015).

3.2.3 Tower Properties

The tower used in the OO-Star Wind Floater is made of conical segments with constant wall thickness. The diameter can be linearly interpolated within each segment. The specific design is described in detail in the technical report Lifes50+ Deliverable D4.2 of Stuttgart (2018), also described in figure 3.3. Important tower parameters are described in table 3.2.

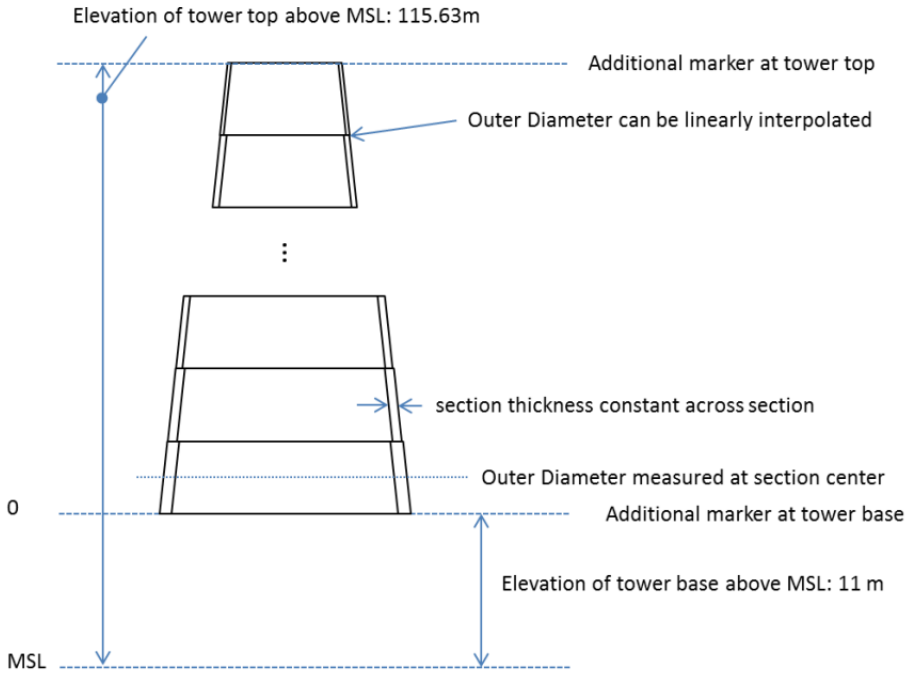

Figure 3.3: Tower definition (of Stuttgart, 2018)

Property	**Value**
Tower base elevation above MSL	11 m
Tower top elevation above MSL	115.63 m
Total mass	$1.257 \cdot 10^6$ kg
1st fore-aft natural frequency, clamped	0.5529 Hz
1st side-side natural frequency, clamped	0.5539 Hz
Density ρ	$8.243 \cdot 10^3$ kg/m
Modulus of elasticity E	$2.1 \cdot 10^{11}$ N/m
Shear modulus of elasticity G	$8.08 \cdot 10^{10}$ N/m

Table 3.2: Tower parameters of OO-Star Wind floater 10MW, adopted from of Stuttgart (2018) and DTU (2018).

The detailed design of each segment is in table 3.3. The tower diameter is defined at the section centre as described in figure 3.3. The model in SIMA has a simplified design of the tower. The tower is modelled with 27 sections with the correct properties for the centre of the segment. The segments are thus modelled with a constant cross-section instead of being conical. This simplification is considered sufficient to capture the effects of the tower natural frequency. It could be necessary to divide the tower up into more segments for the detailed design. The tower segments are defined as beam elements with diameter, thickness, material density, elasticity modulus and shear modulus.

Section	Lower elevation	Upper elevation	Outer Diameter	Wall thickness
1	0 m	3.946 m	11.385 m	0.075 m
2	3.946 m	7.892 m	11.154 m	0.074 m
3	7.892 m	11.838 m	10.923 m	0.072 m
4	11.838 m	15.785 m	10.692 m	0.070 m
5	15.785 m	19.731 m	10.462 m	0.068 m
6	19.731 m	23.677 m	10.231 m	0.066 m
7	23.677 m	27.623 m	10.000 m	0.065 m
8	27.623 m	31.569 m	9.769 m	0.063 m
9	31.569 m	35.515 m	9.538 m	0.061 m
10	35.515 m	39.462 m	9.308 m	0.059 m
11	39.462 m	43.408 m	9.077 m	0.057 m
12	43.408 m	47.354 m	8.846 m	0.056 m
13	47.354 m	51.300 m	8.615 m	0.054 m
14	51.300 m	55.246 m	8.385 m	0.052 m
15	55.246 m	59.192 m	8.154 m	0.050 m
16	59.192 m	63.138 m	7.923 m	0.048 m
17	63.138 m	67.085 m	7.692 m	0.047 m
18	67.085 m	71.031 m	7.462 m	0.045 m
19	71.031 m	74.977 m	7.231 m	0.043 m
20	74.977 m	78.923 m	7.000 m	0.041 m
21	78.923 m	82.869 m	6.769 m	0.039 m
22	82.869 m	86.815 m	6.538 m	0.038 m
23	86.815 m	90.762 m	6.308 m	0.036 m
24	90.762 m	94.708 m	6.077 m	0.034 m
25	94.708 m	98.654 m	5.846 m	0.032 m
26	98.654 m	102.600 m	5.615 m	0.030 m
27	102.600 m	104.630 m	5.441 m	0.029 m

Table 3.3: Tower properties of Stuttgart (2018)

3.2.4 Modified Tower Properties

As specified in 2.3.3, the first tower natural frequency for a soft-stiff tower should be between 0.2-0.28 Hz. Together with supervisors, it was decided that the best way to make the tower more flexible is to reduce the elasticity modulus. By doing this, the new tower design will be identical to the original model, and thus it will give a realistic comparison between the two models. The soft-stiff tower will be referred to as a *flexible tower*, and the stiff-stiff tower as a *stiff tower*.

A simple estimate is done to find a new elasticity modulus that provides the wanted natural frequency. A cantilever beam will have its first natural frequency given by equation 3.1. The original model has a first natural frequency of about 0.5 Hz of Stuttgart (2018), and this should be divided by two. By only changing E, the elasticity modulus should be divided into one quarter of its current value to obtain half the natural frequency according to the simple theory in equation 3.1. This results in a reduction from $E = 210$ GPa to $E = 52.5$ GPa with a corresponding shear modulus $G = 18.462$ GPa. The new properties are summarized in table 3.4. With these values, the first natural frequency is 0.236 Hz for tower side-side and 0.241 Hz for tower fore-aft mode, as displayed in table 3.5. The natural frequencies are found with an eigenvalue calculation in SIMA.

$$\omega_1 = (nL)_1^2 \sqrt{\frac{EI}{mL^4}} \tag{3.1}$$

Elasticity modulus	**Shear modulus**
E	**G**
52.5 GPa	18.462 GPa

Table 3.4: New tower properties for a flexible tower

This tower design is not realistic as there are no steel types with this elasticity modulus. The alternative changes would be to reduce the thickness or diameter. Reduction of thickness alone would require a reduction that is unrealistic and that would most likely lead damage. A quick check was done in SIMA with an eigenvalue analysis and reduction of the wall thickness. It was found that the wall thickness must be thinner than 0.02 meters to archive a soft-stiff natural frequency when the diameter is unchanged. As discussed in section 2.3, this is not feasible because the slenderness ratio will become too high and local

buckling failure can be expected.

Reducing the diameter would lead to changes in the design of the tower bottom connection to the platform. This will change the design of the connection between the concrete shaft and the steel tower. In addition, the tower height can be reduced to change the stiffness by lifting the transition from concrete shaft to the steel tower. The optimal way of reducing the tower natural frequency while maintaining a safe design is probably a combination of changing the diameter, stiffness and height. For now, the material properties will be changed to see if the tower is safe against fatigue failure and ultimate loads. The trend found by this approach will be used to see if further work on the subject will give a satisfactory tower design.

Model:	**Stiff**	**Flexible**
Fore-aft mode [Hz]	0.53883	0.241
Side-side mode [Hz]	0.53881	0.236

Table 3.5: Natural frequency of tower for the tower models (of Stuttgart, 2018)

3.2.5 Controller Properties and Calibration

The controller used in a wind turbine ensures that the turbine is operating correctly and in a safe manner. The model in SIMA is controlled by the general DTU controller and must be modified for the specific wind turbine platform it is used on. The important aspects for the controller in this thesis are to avoid negative damping and amplified tower vibrations.

Negative damping is a problem that occurs if a wind turbine controller made for a bottom-founded structure is used on a floating wind turbine. The reason is related to the motion of the floater compared to the relative wind speed. When the floating wind turbine leans to the front against the wind, the relative wind speed will increase and the thrust will decrease. When the wind turbine lean to the back the opposite will happen. This leads to negative damping and large motions can be induced. The issue is suppressed by including a motion control of the tower and calibrate the controller with the tower frequency (Mikel [Iribas, 2017). With help from Olav Olsen, the specific changes that must be done and calibrated for are found to be:

- **Controller frequency:** should be set to less than the pitch eigenfrequency according to the pole placement method to avoid negative damping.

- **Tower vibrations:** To avoid unacceptable tower vibrations, a speed exclusion zone depending on the tower fore-aft frequency must be included. From the frequency, the rotational speed and generator torque must be calculated. Also, the tower side-side vibrations must be avoided, this is done by introducing a tower side-to-side notch filter with the correct frequency.

The rest of the controller input does not need to change due to the changes made in the model. The other values needed are rated values for the turbine and normal values for the controller. The OO-Star Wind Floater has a constant torque controlled fully loaded generator, which means that the torque should be smooth above rated wind speed.

The speed exclusion zone prevents the generator from operating at speeds which leads to excitation of the tower fore-aft mode. The speed zone is found by calculating the rotor speed from the fore-aft tower natural frequency. From the rotor speed, the corresponding generator torque can be found as in equation 3.2. In this equation, the generator torque τ_{gen} can be found for the low and high rotor speed limits Ω with use of the optimal C_p tracking factor k (Mikel [Iribas, 2017).

$$\tau_{gen} = k\Omega^2 \tag{3.2}$$

The speed exclusion zone is typically set to $\pm 10\%$ of the first tower fore-aft frequency. A higher percentage leads to even less tower vibration amplifications, but also to less power output of the turbine. A narrower zone gives a higher power output from the turbine, but also increases the tower displacement and thus leads to higher fatigue loads (Licari et al., 2013).

Figure 3.4 illustrates how the speed exclusion zone for the generator works. The torque is kept constant over the area defined as the exclusion zone to avoid rotational speeds close to the tower frequency. The value of the constant torque is different depending on increasing or decreasing speed. Thus, both low-speed and a high-speed limit must be defined.

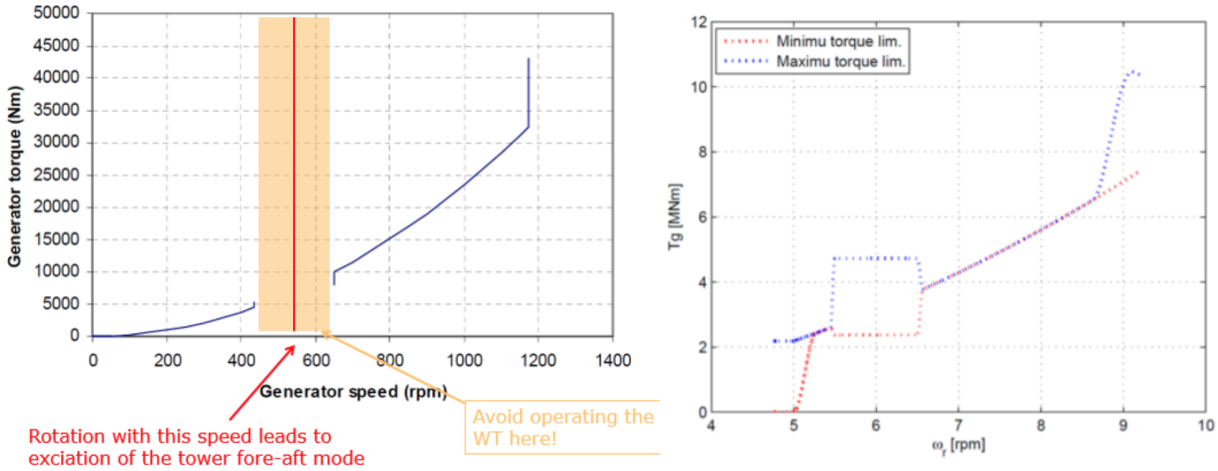

(a) Speed exclusion zone

(b) Torque limits

Figure 3.4: Illustration of the speed exclusion zone, provided by Jonas Gullaksen Straume, Dr. Techn. Olav Olsen.

The controller file is in appendix A. A Campbell diagram is used to see if a speed exclusion zone is necessary, this is in section 3.4.3. The tuning of the controller is based on information provided by Jonas Gullaksen Straume in Dr. Techn. Olav Olsen. Some calculations are done to get a basis for the parameters. Then testing and tuning by trying different values is done. The behaviour was checked with constant wind tests and by ensuring that negative damping is avoided.

3.3 Site Conditions

The project Lifes50+ investigated three sites for the analysis of floating wind turbines. The difference between the sites was mainly the severity of the environmental conditions, from moderate to medium to sever met-ocean conditions. The choice of site was the medium conditions, which also had the largest water depth. This is based on the Gulf of Maine in the United States of America (Pablo Gomez, 2015). Table 3.6 gives the properties of the site. The specific environmental values for each analysis is given in the section describing the analysis type. The design water depth is 130 meters. The chosen design load cases for FLS and ULS are based on statistics from measurements at the site.

50 year wind at hub	**50 year significant wave height**	**50 year peak period**	**Extreme water level**	**Soil**	**Water depth**
44 m/s	10.9 m	9-26 s	4.3 m	Sand Clay	50-130 m

Table 3.6: Met-ocean conditions of the Gulf of Maine (Pablo Gomez, 2015)

In the analysis for FLS and ULS, the wind and waves are assumed to be aligned at all times. This is a simplification with varying impact on the results. In L. Barj (2014), it was seen that the misalignment has a "considerable impact on the side-side loading for both ULS and FLS conditions". In addition, it was found that the side-side tower fatigue damage was under predicted while the fore-aft damage was over predicted with aligned wind and waves. In Kvittem and Moan (2015), it was found that aligned wind and wave condition gave the most conservative loads and that the substructure is more dependent on the load direction than the tower and blades. Also in Bachynski et al. (2014), the aligned conditions gave the most conservative loads on the tower. Based on the research, it was therefore chosen to use aligned conditions to find the most conservative loads in the fore-aft direction. An evaluation of the impact in the side-side direction should be done based on the results.

3.4 Validation and Calibration of the Model

This section explains briefly the steps done for validating the SIMA model and the calibrations done for a correct result. Firstly, the turbine and controller performance is tested with constant wind tests to check the behaviour. Secondly, the platform motions and hydrodynamic properties are tested with decay tests. At last, the modes of the tower and blades are identified to find eigenvalues and calibrate the controller.

3.4.1 Validation of Wind Turbine Performance

The DTU 10MW reference wind turbine model is checked to validate the performance of the turbine and controller. This is done by performing constant wind tests. The tests are carried out by time-domain analysis with no waves and uniform constant wind speeds from 3 m/s - 22 m/s. The tests are done with a fixed platform to avoid transients and thus avoid a long simulation length. The performance found is compared to the reference results for the turbine in DTU (2015).

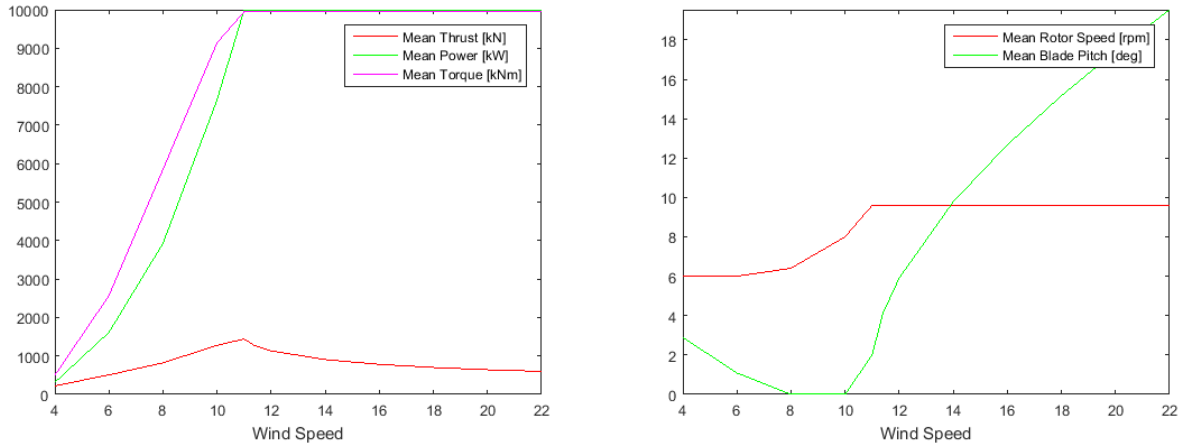

(a) Rotor thrust, power and torque

(b) Rotor speed and blade pitch

Figure 3.5: Constant wind test for the wind turbine and controller

Figure 3.5 gives the obtained values from the constant wind tests. The startup time for the rotor is not included. The torque and power reach its maximum at the correct value at the rated wind speed. The rotor speed is constant above rated wind speed. The thrust is increasing until rated wind speed and decreasing after, as expected. The blade pitch is correct and used to change the thrust to have constant torque and power. The wind turbine with the blades provided by Sitan Sørum is therefore considered to operate correctly.

3.4.2 Validation of Platform Behaviour

Free decay tests are used to find natural periods of the platform to compare to literature to check the behaviour of the platform. The tests are performed for all six degrees of freedom individually. The wind turbine is parked during the simulations to reduce the degrees of freedom and coupling. The tests are done by applying a force or moment from zero until a specified ramp force, hold the force constant for some time and then release it. This is done without wind and wave. The platform will then oscillate and the motion will be damped out. From this, it is possible to fit damping parameters to the oscillatory motion to estimate the damping and find the natural period.

The damping coefficients are not found because no reference values are found. The results form SIMA are post-processed in MATLAB and the toolbox WAFO (Brodtkorb et al., 2000) is used to find the natural frequency for each motion by counting of peaks and troughs of the motion. The results are presented in table 3.7. Figure 3.6 displays the decay test done for the surge motion, where the blue line gives the motion and the red line is fitted with damping coefficients and damping period.

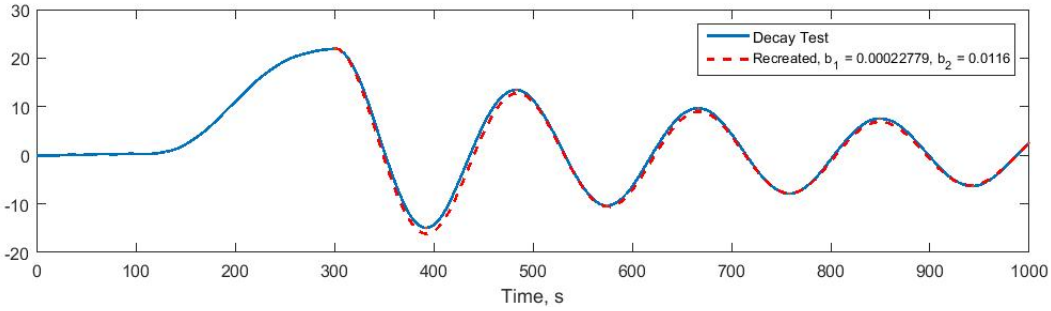

Figure 3.6: Decay test for surge motion

.

Degree of freedom	Stiff-stiff $T_n[s]$	Stiff-stiff $f_n[Hz]$	Soft-stiff $T_n[s]$	Soft-stiff $f_n[Hz]$	Reference $[Hz]$
Surge	183.4	0.00545	179.9	0.00559	0.0054
Sway	183.2	0.00546	179.1	0.00558	
Heave	20.84	0.048	19.81	0.050	0.0478
Roll	31.84	0.0314	32.2	0.031	
Pitch	31.82	0.03143	30.97	0.032	0.0318
Yaw	98	0.010	95.8	0.010	0.0097

Table 3.7: Natural period and frequency from decay tests for all six degrees of freedom DTU (2018)

It is seen that the obtained natural frequencies from decay tests are similar to the reference values from DTU (2018). As expected, sway and roll values are similar to surge and pitch due to symmetry. The largest offset is for yaw motion. The reference results are calculated in the program FAST8 for a rigid platform. Differences in the modelling of the platform could be the reason for the offset in value. Based on the decay tests, the model of the platform and floater can be expected to behave correctly in SIMA. It is also seen that there are small differences between the stiff-stiff model and the soft-stiff. This indicates that the flexibility of the tower influences the natural frequencies of the platform motions. A spectral analysis of the platform motions will be used to investigate the significance of the difference.

3.4.3 Campbell Diagrams

A Campbell diagram for wind turbines plots the natural frequencies of the system against the rotational speed. The natural frequencies can depend on the rotation, and this is accounted for in a Campbell diagram. The natural frequencies are seen in conjunction with the rotational frequencies of the turbine to check for possible resonance behaviour.

A diagram is made for both of the models with an eigenvalue analysis in SIMA. The diagram made is simplified as it does not account for the natural frequencies dependency on rotor speed, and they are assumed to be constant. The tower fore-aft and side-side natural frequencies are quite independent of the rotor speed, so the simplification will not affect the tower frequency resonance check (M Jonkman and J Jonkman, 2016). The diagram is used to check where the frequencies of the system are crossing the xP ranges for rotor speed operational area and the different xP ranges. The rotor speed is varied between

6-9.6 rpm and the xP ranges are dependent on the rotor speed. The critical aspects are:

- **Tower frequencies:** must not cross the 1P and 3P lines. If they are close, the speed exclusion zone can be activated to avoid rotations which can amplify the tower vibrations.
- **Energy content:** The different xP modes have varying energy content, which will influence the impact the mode represents. It is also important to check if the mode represents a danger of resonance in the low or high rotor speed area. From cut-in speed till rated wind speed, the rotor will be in low speed, while after rated wind speed, the rotor speed will be at its highest speed. It is expected to be the frequencies crossing at high rotor speed that is most critical as the turbine is expected to be operating more at maximum rotor speed compared to the lower rotor speeds.

Figure 3.7 and 3.8 gives the obtained Campbell diagrams for the stiff-stiff and soft-stiff model. The area in between the black vertical lines represents the operational area of the turbine. Crossings of 1P and 3P frequency is considered the most fatal and present danger of resonance because these rotational frequencies have a high amount of energy. 6P and 9P can also contain a significant amount of energy, an crossing with these should be evaluated (M Jonkman and J Jonkman, 2016). The DNV criteria of frequency avoidance of ±5% are not accounted for in the diagram and must be considered.

The stiff-stiff original model has a side-side 1st natural frequency close to the 3P frequency at a high rotation speed. The frequency is not outside the ±5% range of allowance, and the speed exclusion zone must be activated. The rotor edgewise frequencies cross the 6P frequency at the rotor startup, while the flapwise are crossing 6P at high rotor speed and 9P at low rotor speed. Resonant behaviour from the blade modes can also be avoided with use of active control (M Jonkman and J Jonkman, 2016) if the controller is calibrated for this. This is not investigated in this thesis as it is the tower that is in focus.

The tower natural frequencies for the soft-stiff tower is well within the allowed ranges stated by DNV, this is seen in figure 3.8. The first rotor edgewise symmetrical frequency crosses the 3P at maximum rotor speed. It is thus decided to have the same speed exclusion zone as for the stiff-stiff model to avoid resonant behaviour from this natural frequency in the model.

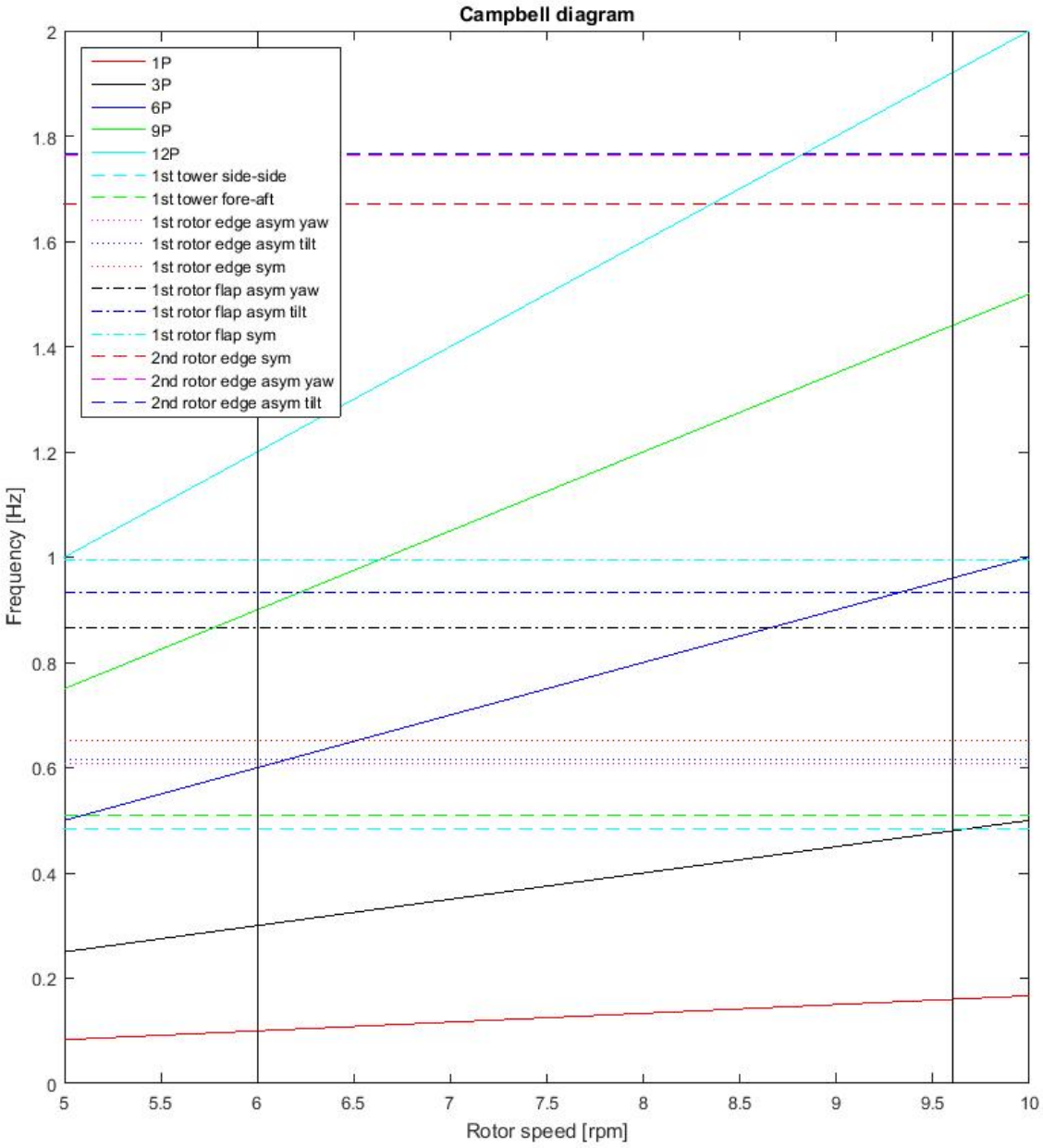

Figure 3.7: Campbell diagram for stiff tower model

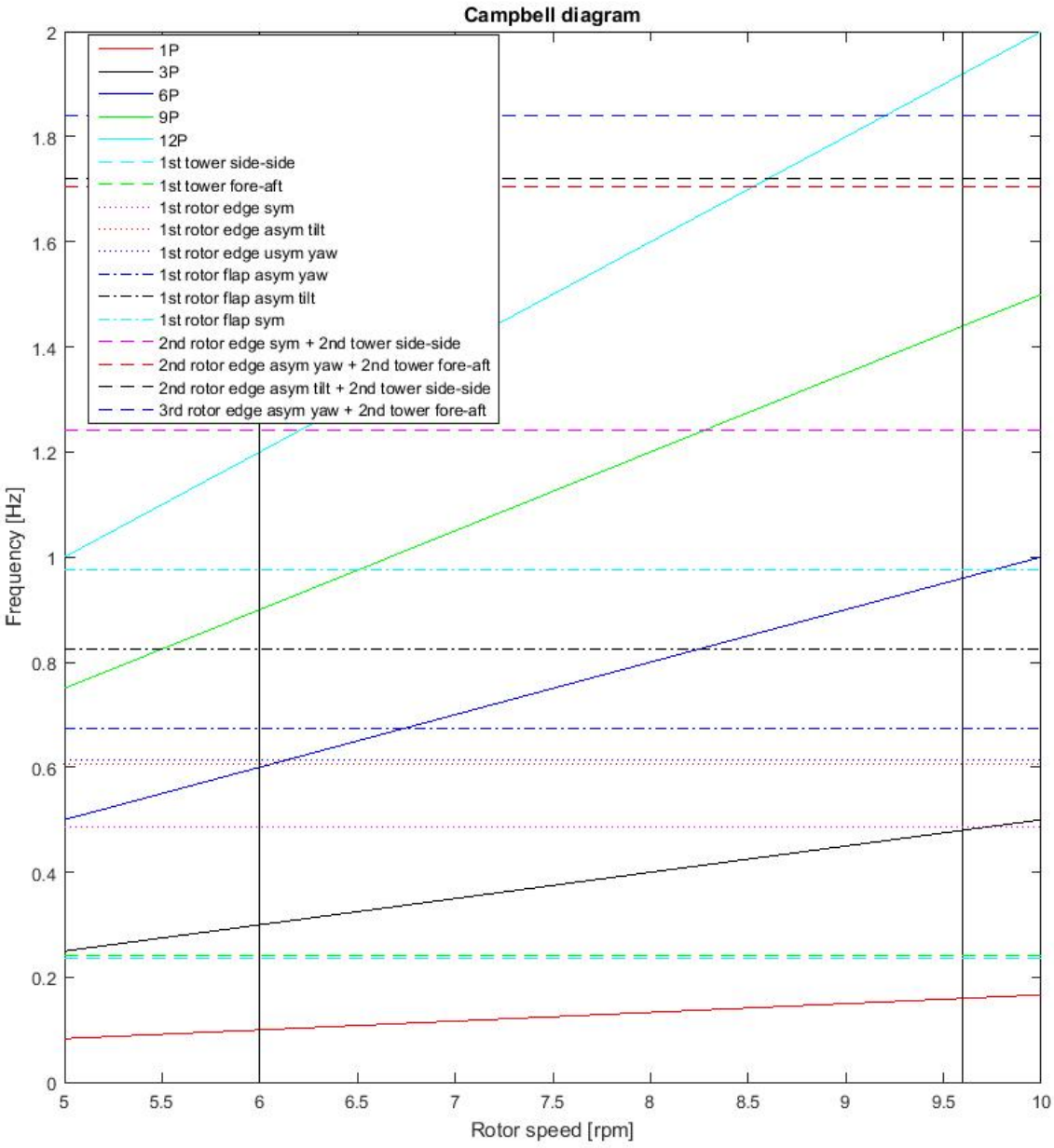

Figure 3.8: Campbell diagram for flexible tower model

3.5 Fatigue Limit State Analysis

"The aim of a fatigue design is to ensure that the structure has sufficient resistance against fatigue failure" (DNV, 2014). Fatigue is the phenomenon occurring "when a material is weakened due to repeatedly applied loads" (Stavridou et al., 2015). The weakened material is subject to crack initiation and propagation at local regions that experience a stress concentration. This occurs from repeated loading and unloading of susceptible areas. First, microscopic cracks arise at the stress concentration area before the crack suddenly propagate and the structure can collapse without prior notice. Susceptible areas for fatigue are welds, thickness changes, holes, sharp edges and other structural details (Stavridou et al., 2015). The fatigue life of a structure depends on the possibility for inspection and testing of structural details to detect crack initiations and estimate the time until crack propagation.

Wind turbine towers on a floating platform are subjected to stresses that are applied and relaxed repeatedly due to both wave- and wind loading. Tower details like "local connections, welds, bolts and shell thickness variations are vulnerable to developing fatigue failure" (Stavridou et al., 2015). The tower consists of segments with different thickness. In this fatigue analysis, the welded connection between the segments with changing thickness will be studied since these are advised to be checked by DNV.

Fatigue life is "defined as the number of stress cycles of a specified character that a structural detail can sustain before failure occurs" (Stavridou et al., 2015). From sample tests, the maximum allowed number of each individual stress range is found to avoid fatigue damage. The samples can resist a larger number of small-ranged stress cycles compared to large range stress cycles.

3.5.1 A Priori Estimation of Fatigue Damage of Flexible Tower

A more flexible tower is expected to experience more and larger vibrations. This will increase the number of stress cycles during the lifetime of the structure. Because of this, more fatigue is expected for a flexible tower than a stiff tower.

The tower base is expected to experience most fatigue damage because the bending moments are largest in the base. A linear decrease in damage is common from the base to the tower top, but the damage can be significant in areas with a large cross-sectional change or high loads along the tower (Erin E. Bachynski, 2015).

Four points at the tower cross-section are of interest. These points are at the fore-aft and side-side axis

lines and are of particular interests because they are expected to show the fatigue damage variation and proportion. The fore-aft points are in the direction of the aligned wind and waves, and will therefore experience the largest loads. The side-side damage is used to check for resonance and see the difference from the fore-aft damage. Due to the assumption that aligned wind and wave conditions will give a conservative result, there is a possibility that the tower side-side damage is under predicted.

3.5.2 Fatigue Calculation

The fatigue damage calculation is based on S-N curves. An S-N curve describes the relationship between stress range S and the number of stress cycles N. The curve is made with test samples that are loaded until fatigue failure occurs. The curve is adjusted to a mean minus two standard deviations to ensure a 97.7% probability of survival.

The failure criterion is based on checking if the amount of each individual stress range during the structures lifetime is less than the number of cycles allowed in the S-N curve. The characteristic cumulative damage is based on Miner's rule. This assumes linear cumulative damage. The stress range history is used to sum up the number of cycles, this is usually done with rainflow counting method. D_C is the characteristic cumulative damage and is defined as in equation 3.3.

$$D_C = \sum_{i=1}^{I} \frac{n_{C,i}}{N_{C,i}} \tag{3.3}$$

in which

I = total number of stress range blocks

$n_{C,i}$ = number of stress cycles in the i'th stress block

$N_{C,i}$ = Number of cycles to failure at stress range of the i'th stress block

The design cumulative damage D_D is found by multiplying D_C with the design fatigue factor DFF as in equation 3.4.

$$D_D = DFF \cdot D_C \tag{3.4}$$

The stress range history is found from the fatigue analysis. The stress range that is found gives the nomi-

nal stress calculated from classical theory. For a tubular structure, it is the hot spot stress that is relevant for fatigue life. Hot spot stress is the stress experienced in a structural area with a stress concentration. The hot spot stress is found in equation 3.5. The method is based on establishing a stress concentration factor (SCF), that is dependent on the structural detail in question and found from parametric equations in the standard DNV-RP-C203.

$$\sigma_{hotspot} = SCF \cdot \sigma_{nominal} \tag{3.5}$$

The nominal stress is only found as axial stress and shear stress is neglected. According to Kvittem and Moan (2015), the fatigue damage resulting from shear stress is negligible compared to the axial stress. Equation 3.6 gives the nominal axial stress calculated from the analysis in SIMA. In this equation, N_z is the axial force, A is nominal cross-section area, M_y and M_z are bending moments and I_y and I_z are sectional moments. r is the cross-section radius and θ is the angle starting from the wind-wave direction and moving in the counterclockwise direction. M_y is the fore-aft bending moment and M_z is the side-side bending moment. For aligned wind and wave, it is the points $\theta = 0°$ and $\theta = 180°$ that is expected to experience most fatigue damage. This is because the fore-aft moment is expected to be the largest and most variable because of the simultaneous wind and wave environment in this direction.

$$\sigma_{nominal} = \frac{N_z}{A} + \frac{M_y}{I_y} \cdot r \cdot cos\theta - \frac{M_z}{I_z} \cdot r \cdot sin\theta \tag{3.6}$$

The criterion for a safe fatigue design is set by equation 3.7.

$$D_D \leq 1.0 \tag{3.7}$$

The calculation is done in MATLAB with use of the toolbox WAFO (Brodtkorb et al., 2000). First, the nominal stress is calculated for all tower segments and the stress concentration factor is multiplied to find the hot spot stress. Then the number of stress cycles for each range is found by use of the rainflow counting routine in WAFO. The WAFO toolbox is also used to calculate the fatigue damage for each tower segment by use of the chosen S-N curve. The S-N curve is modified from the WAFO routine to include two slopes. The fatigue damage is found for each load case and the probability of occurrence for each DLC is used to find the total damage for 1 hour. The total lifetime fatigue is calculated by multiplying the one hour damage with $24 \cdot 365 \cdot 25$ to find the damage for 25 years.

3.5.3 Stress Concentration Factor

A stress concentration factor (SCF) is multiplied to the number of stress ranges to ensure a safe and conservative design. DNV-RP-C203 defines an SCF as "the ratio of hot spot stress range over nominal stress range". Hot spot stress is the stress found in structural details, for example a part of a weld. The nominal stress is the theoretical stress found in the section and will be the range found in fatigue analysis in SIMA. The SCF will be multiplied to the nominal stress found in analysis to account for a stress concentration in the structural detail studied.

According to **?**, the tower sections with different wall thickness is connected with butt welds. The SCF for butt welds at thickness transitions at girth welds in tubulars are given in DNV-RP-C203 section 3.3.7.3. Equation 3.8 with equation 3.9 and 3.10 give the calculation routine for the stress concentration factor. It is assumed that the thickness reduction of the tower is on the inside of the tubular and that the weld is only made from the outside as in figure 3.9. These assumptions are conservative and a different weld could reduce the SCF.

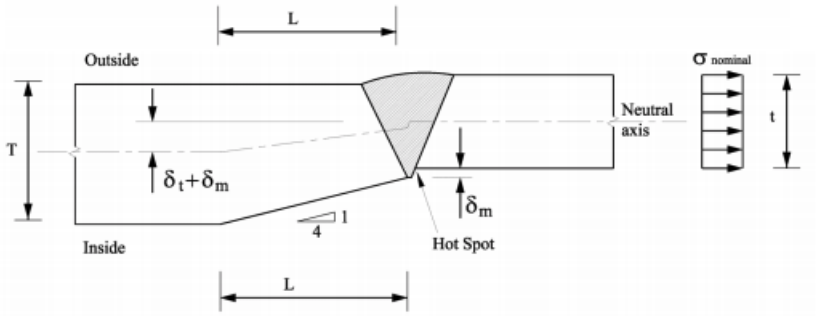

Figure 3.9: Detail of geometry for weld in tubular from the outside from DNV-RP-C203

$$SCF = 1 + \frac{6(\delta_m + \delta_t - \delta_0)}{t} \frac{1}{1 + \left(\frac{T}{t}\right)^{\beta}} e^{-\alpha} \tag{3.8}$$

$$\alpha = \frac{1.28L}{\sqrt{Dt}} \frac{1}{1 + \left(\frac{T}{t}\right)^{\beta}} \tag{3.9}$$

$$\beta = 1.5 - \frac{1}{log\left(\frac{D}{t}\right)} + \frac{3}{\left(log\left(\frac{D}{t}\right)\right)^2} \tag{3.10}$$

Table 3.8 gives an explanation of the parameters used in equation 3.8-3.10. The formulas for the param-

eters are based on standard values used in DNV-RP-C203 and fabrication standards.

Symbol	Description	Formula
δ_m	Maximum eccentricity misalignment	$0.15t$
δ_t	Eccentricity due to change in thickness	$\frac{1}{2}(T-t)$
δ_0	Eccentricity inherent in the S-N curve	$0.05t$
t T	Thickness of smaller and larger tubular	-
L	Length of eccentricity	$4(T-t)$
D	Outer tubular diameter	-

Table 3.8: SCF values explained, DNV-RP-C203

The SCF for the bottom of the tower is assumed to be based on the transition between the concrete central column and the tower interface. The central column has a diameter of 12.05 m at the interface with an unknown thickness. It is therefore assumed a conservative value with results in a high SCF of 1.6 for a thickness of 0.6 m for the central column.

3.5.4 Design Fatigue Factor

According to DNV-OS-J101, wind turbine towers should be designed for a DFF = 2. This is based on the tower being in air with coating, and assume that the coating will be repaired throughout the lifetime.

3.5.5 S-N Curve

The S-N curve is based on equation 3.11 and has two areas with a linear relationship, displayed in figure 3.10. Different S-N curves are made for structures in air, in seawater and with or without cathodic protection. According to DNV-RP-C203, it has been common practice in Norway to use seawater S-N curve with cathodic protection for joints in the splash zone. It is then assumed that the joints have a good coating. This can also be assumed to be representative of the wind turbine tower, and it is a conservative decision compared to using S-N curves in air.

$$log_{10} = log_{10}a - mlog_{10}\left(\Delta\sigma\left(\frac{t}{t_{ref}}\right)^k\right) \tag{3.11}$$

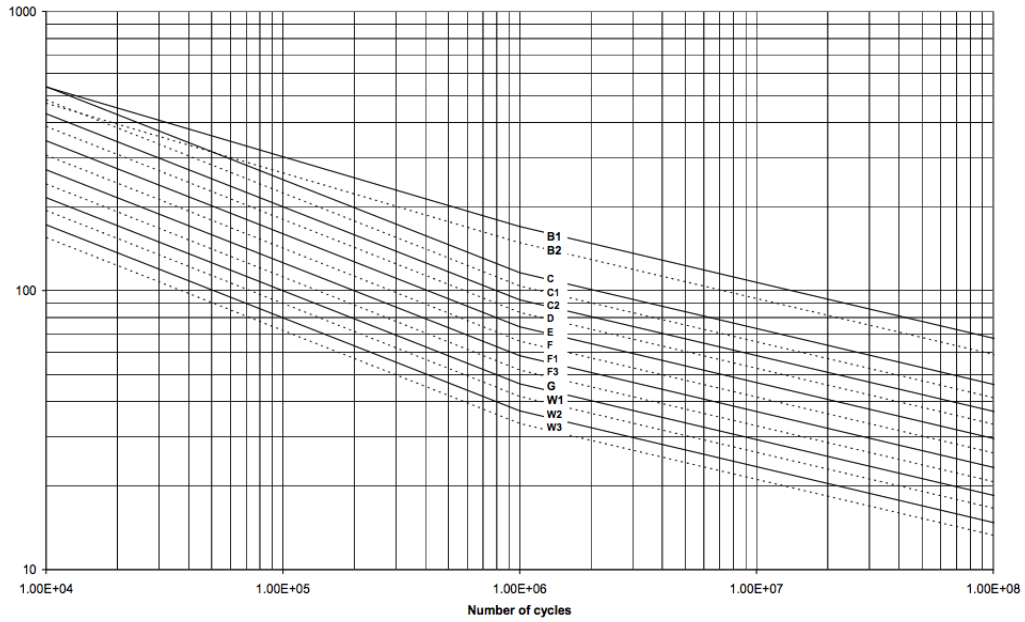

Figure 3.10: S-N curve in seawater with cathodic protection from DNV-RP-C203

Different curves are made for different structural details. A butt weld at tubular girth weld is described with curve F3 for weld root and D for weld toe. F3 has a lower S-N curve and thus a lower allowed range of stress cycles. It was therefore decided to look at the weld root. The properties for the F3 S-N curve are given in figure 3.11.

S-N curve	$N \leq 10^6$ cycles		$N > 10^6$ cycles	Fatigue limit at 10^7 cycles (MPa) *)	Thickness exponent k	Structural stress concentration embedded in the detail (S-N class), see also equation (2.3.2)
	m_1	$\log \bar{a}_1$	$\log \bar{a}_2$ $m_2 = 5.0$			
B1	4.0	14.917	17.146	106.97	0	
B2	4.0	14.685	16.856	93.59	0	
C	3.0	12.192	16.320	73.10	0.05	
C1	3.0	12.049	16.081	65.50	0.10	
C2	3.0	11.901	15.835	58.48	0.15	
D	3.0	11.764	15.606	52.63	0.20	1.00
E	3.0	11.610	15.350	46.78	0.20	1.13
F	3.0	11.455	15.091	41.52	0.25	1.27
F1	3.0	11.299	14.832	36.84	0.25	1.43
F3	3.0	11.146	14.576	32.75	0.25	1.61
G	3.0	10.998	14.330	29.24	0.25	1.80
W1	3.0	10.861	14.101	26.32	0.25	2.00
W2	3.0	10.707	13.845	23.39	0.25	2.25
W3	3.0	10.570	13.617	21.05	0.25	2.50

Figure 3.11: S-N curve values in seawater with cathodic protection from DNV-RP-C203

3.5.6 Design Load Cases for FLS

Design load cases for FLS are set up in the project Lifes50+ *Deliverable D4.5 State-of-the-art models for the two Lifes50+ 10MW floater concepts* (DTU, 2018). Table 3.9 give the properties of the 7 design load cases chosen for fatigue analysis based on a high probability of occurrence. These load cases are determined to give a representative result for testing the model in the environment in the Gulf of Maine in the US. The environment is described with a Pierson-Moskowitz spectrum for the irregular sea state and wind turbulence of class C described with a Kaimal spectrum. All fatigue load cases are with an operational turbine and active control by the controller. The load cases are presented in Table 3.9. Each load case is run in SIMA for 5400 seconds in the time domain, where the first 1800 s are removed because of transients. The turbulent wind state is described with turbulence boxes with a duration of 5400 seconds.

State number	Waves	Wind	Wind seeds	Wind turbine	Probability
FLS 1	$H_s = 1.38$ m $T_p = 7$ s	5 m/s	-382116359, 740207055	Operating Active control	0.0689%
FLS 2	$H_s = 1.67$ m $T_p = 8$ s	7.1 m/s	-1772244974, -1723525961	Operating Active control	0.1198%
FLS 3	$H_s = 2.20$ m $T_p = 8$ s	10.3 m/s	-190776590, -1657303509	Operating Active control	0.1283%
FLS 4	$H_s = 3.04$ m $T_p = 9.5$ s	13.9 m/s	-1730267664, -825240408	Operating Active control	0.1024%
FLS 5	$H_s = 4.29$ m $T_p = 10$ s	17.9 m/s	-1689773379, 376850410	Operating Active control	0.0581%
FLS 6	$H_s = 6.20$ m $T_p = 12.5$ s	22.1 m/s	-2136222709, -1568860497	Operating Active control	0.0188%
FLS 7	$H_s = 8.31$ m $T_p = 12$ s	25 m/s	-2136222709, -1568860497	Operating Active control	0.0037%

Table 3.9: Design Load Cases for fatigue limit state analysis (of Stuttgart, 2018), (DNVGL, 2015)

The wave environment is given as input in SIMA. Currents are neglected because they are not considered to contribute to fatigue life. Currents are given as stationary in fatigue analysis and are therefore not expected to contribute to variations in stress in the tower. The turbulent wind is simulated with the

program TurbSim and described as normal turbulence. The turbulent wind files are then included in SIMA as *TurbSim Fluctuating Three Component* wind environment. An example of a TurbSim input file is in appendix B.

According to DNV standard DNV-OS-J101, at least 3 different combinations of wave seeds must be used for each design load case to simulate different start positions of the waves. In this thesis, only one combination is used because only the trend of motions and forces are looked into. For a complete and detailed fatigue analysis, at least three combinations should be used.

3.6 Ultimate Limit State Analysis

The ultimate limit state is based on limiting the maximum stress the material experiences and is thus linked to extreme environmental conditions. The ultimate limit state analysis of an offshore wind turbine should consist of the following checks:

- Ultimate strength analysis: Check if the yield limit is exceeded for the material.
- Stability analysis: Check for local buckling
- Critical deflection analysis: Check the interface between blade and tower to ensure sufficient blade-tip clearance.

3.6.1 Ultimate Strength Analysis

The ultimate strength analysis is based on maximum distortion energy theory, also called the von Mises yield criterion. The theory is valid for ductile materials and states that yielding occurs when the stress reaches a yielding level found in a simple tension test.

Von Mises stress is found by combining principal stresses at critical points in the tower. The theory assumes small deformations and thus a linear theory of elasticity. The von Mises stress σ_v is found directly as output from SIMA analysis. In addition, a material factor is applied according to the ULS criterion in DNV-OS-J101. For a welded connection, a material factor of $\gamma_M = 1.25$ should be applied. The von Mises yield criterion is described in equation 3.12 and checks if the von Mises stress is less than the yield stress σ_y with a material factor to lower the yield limit.

$$\sigma_v \cdot \gamma_m \leq \sigma_y \tag{3.12}$$

Due to a lack of information regarding which steel type is used for the wind turbine tower in this case, the common type S355 is chosen to be used in the design check. Steel type S355 has a yield strength $\sigma_y = 355$ MPa. It is possible to use higher class steel with higher yield strength, but this will increase the steel costs. The soft-stiff tower is made flexible by lowering the elasticity modulus to a level not realistic for steel. It is therefore assumed that the flexible tower has the same yield strength as the stiff tower, but the stresses that are obtained in each tower model will be compared.

3.6.2 Stability Analysis

The stability analysis checks if the structure can experience unstable condition under extreme loading. When a structure fails due to instability, it is called buckling. It is not possible to do a stability calculation on a coupled RIFLEX model in SIMA. The buckling check is thus done with simple formulas to identify if buckling should be investigated further.

For the buckling analysis, DNV-CG-128 and DNV Classification Notes - No. 30.1 are used. The tower is simplified to a beam with a fixed bottom and a free tower top. The tower is subjected to both axial loading and bending, and is thus classified as a beam-column for the calculation.

The buckling analysis is based on finding a usage factor η which is checked against the criterion in equation 3.13. The usage factor defines the relation between the load applied divided by the ultimate load, and a material factor is added to increase the safety margin. The material factor is set to $\gamma_m = 1.15$ as defined in the standards.

$$\eta \leq \eta_{allowed} = \frac{1}{\gamma_m} \tag{3.13}$$

For a beam-column with both axial load and load from bending, equation 3.14 gives the usage factor. Equation 3.15-3.18 gives the calculation of the parameters necessary to find the usage factor for a beam-column. A circular hollow cross-section is defined to be curve *a* for the buckling curves in DNV Classification Notes - No. 30.1, which gives $\lambda_0 = 0.2$ and $\alpha = 0.2$.

$$\eta = \frac{\sigma}{\sigma_{cr}} = \frac{\sigma_a}{\sigma_{a,cr}} + \frac{\alpha\sigma_b}{\left(1 - \frac{\sigma_a}{\sigma_E}\right)\sigma_{b,cr}} \tag{3.14}$$

in which

σ_a = Axial stress due to compression

$\sigma_{a,cr}$ = Characteristic buckling stress for axial compression

σ_b = Effective axial stress due to bending

$\sigma_{b,cr}$ = Characteristic buckling stress for pure bending

σ_E = Euler stress

α = Coefficient depending on type of structure and slenderness ratio

First, the reduced slenderness λ must be established as in equation 3.15. This is found to be above $\lambda = 0.2$, and equation 3.16 is thus used to find the characteristic buckling stress for axial compression $\sigma_{a,cr}$.

$$\lambda = \sqrt{\frac{\sigma_F}{\sigma_E}} \geq \lambda_0 = 0.2 \tag{3.15}$$

$$\sigma_{a,cr} = \sigma_F \cdot \frac{1 + \mu + \lambda^2 - \sqrt{(1 + \mu + \lambda^2)^2 - 4\lambda^2}}{2\lambda^2} \quad \mu = \alpha(\lambda - \lambda_0) \tag{3.16}$$

Here, σ_F is the yield stress and the Euler stress $_E$ is found by equation 3.17. The effective length l_e is defined by the unsupported length l and a effective length factor K. K is set to be 2.1 because the tower is unsupported in the top, as recommended in the standards. In addition, the radius of gyration i is used with area and second moment of area for the cross-section.

$$\sigma_E = \frac{\pi^2 E}{\lambda_k} \quad \lambda_k = \frac{l_e}{i} \quad l_e = K \cdot l \quad i = \sqrt{\frac{I}{A}} \tag{3.17}$$

The characteristic buckling stress for pure bending for a hollow circular is defined in equation 3.18. σ_a and σ_b are found in SIMA by extracting the stresses. The stresses are extracted at the tower bottom, middle and top. The beam studied should be simplified to the lowest second moment of inertia I, but because of very different $\frac{D}{t}$ ratios of the tower sections, three areas are checked to find the worst case.

$$\sigma_{b,cr} = \sigma_F \tag{3.18}$$

In the buckling check, the correct E is used for the two models. The yield stress is assumed to be the 355 MPa for both models.

3.6.3 Critical Deflection Analysis

The critical deflection analysis will investigate the blade-tip clearance to the tower. The necessary values are found as output in SIMA. DNV-OS-J102 gives a criterion for tower clearance in equation 3.19.

$$D_d \leq \frac{D_i}{\gamma_n \gamma_m} \tag{3.19}$$

In which,

D_d = Largest tip deflection when passing the tower

D_i = Smallest distance form the blade tip to tower in the unloaded condition

γ_n = Failure factor

γ_m = Material factor

The material factor γ_m is 1.1, and the failure factor γ_m is 1 for tower clearance. From Christian Bak (2013b), it is found that the unloaded distance between the blade tip and tower is at least 15 meters, accounting for a larger tower than in the report. The blade tip out-of-plane deflection is used to find the blade deflection towards the tower in SIMA.

3.6.4 Design Load Cases for ULS

The design load cases for ULS is also defined in *Deliverable D4.5 State-of-the-art models for the two Lifes50+ 10MW floater concepts* (DTU, 2018). Table 3.10 gives the parameters for the 3 design load cases. Two are with operating wind turbine and severe wave environment. The last one is with a parked turbine and extreme wind speed. The maximum wind speed is with 50-year return period, as stated in the standard to be necessary. The wave environment is defined with 50-year significant wave height and peak period.

State number	Waves	Wind	Wind seeds	Wind turbine
ULS 1	H_s = 10.9 m T_p = 16 s	7.1 m/s	-401347869, 563291184	Operating Active control
ULS 2	H_s = 10.9 m T_p = 16 s	22.1 m/s	172367112, -140113276	Operating Active control
ULS 3	H_s = 10.9 m T_p = 16 s	44 m/s	-403456158, -941310765	Parked Blades feathered

Table 3.10: Design Load Cases for ultimate limit state analysis (of Stuttgart, 2018)

Also for the ULS analysis, the environment is described with a Pierson-Moskowitz spectrum for the irregular sea state and wind turbulence of class C described with a Kaimal spectrum. Each load case is run in SIMA for 5400 seconds in the time domain, where the first 1800 s are removed because of transients. The turbulent wind field is made with TurbSim. The standards require a 3-hour simulation of extreme conditions, but to limit the simulation length only 1 hour is done in the analysis. One hour simulation length should be sufficient to check for possible ultimate limit failures.

3.7 Spectral Analysis

A spectral analysis is used to estimate the power spectrum of a signal from its time-domain representation. The analysis transforms the time-domain into the frequency-domain, to see signal characteristics that are difficult to analyze in the time-domain. The time-domain show how a signal changes over time, while the frequency-domain show how the signal's energy is distributed over a range of frequencies (MathWorks, 2019).

In this thesis, the power of the signal will be measured in the spectral analysis. To do this, a power spectral density (PSD) or a power spectrum is found by normalizing the output from the signal. "The PSD describes how the power of a time signal is distributed with frequency" (MathWorks, 2019). It is possible to reduce noise from the signal by smoothing the spectrum, this is not done to avoid losing signals. A PSD spectrum is found for the platform motions and the tower bottom bending moments to check for coupled behaviour and resonance. The largest PSD value is expected to be at the natural frequency of the signal. It is possible to check for amplification at the rotor rotational frequencies and see if resonance is avoided in these frequency areas. Power amplification can also originate from wind or wave climate. The WAFO toolbox is used to transform the time-domain into a PSD-frequency spectrum (Brodtkorb et al., 2000).

Chapter 4

Results and discussion

4.1 Fatigue Limit State assessment

This section will present the results from the fatigue limit state analysis. The total lifetime damage is illustrated and the design load cases are assessed to see which contribute to the most damage. The results will be discussed continuously throughout the section.

4.1.1 Fatigue Damage Results

Figure 4.1 gives the total fatigue damage over the tower height for 25 years of operation. It is assumed that the turbine is only in operating condition its entire lifetime and that the 7 design load cases are representative of the environment of 25 years. Only aligned wind and wave conditions are studied. The assumptions will be discussed in relation to the results.

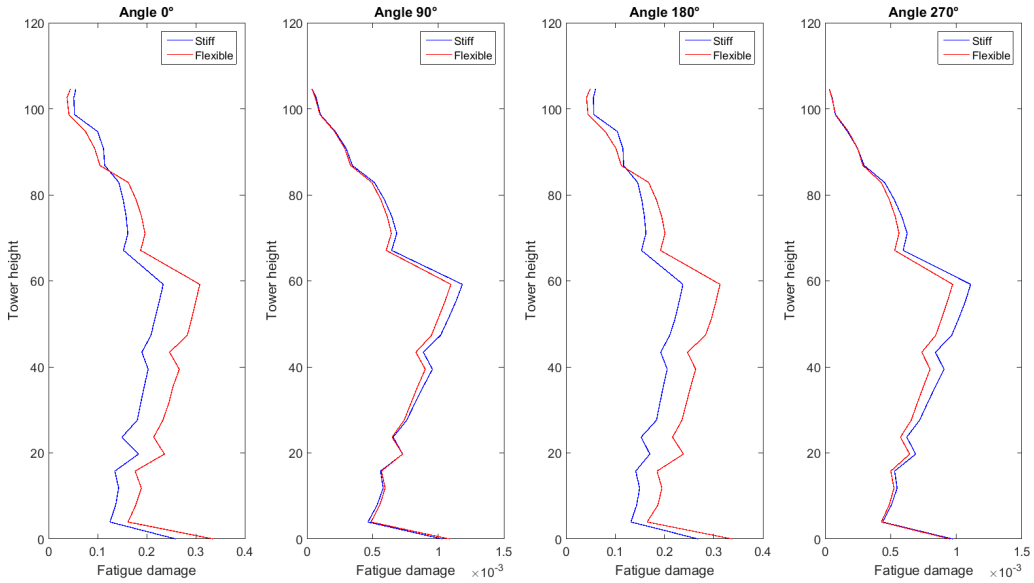

Figure 4.1: Design cumulative damage for 25 years along the tower height for four points on the tower cross-section

From figure 4.1, several interesting features are seen that should be discussed to understand the fatigue loading and the influence of a flexible tower. The following aspects will be looked into:

- The amount of design cumulative fatigue damage D_D
- The difference between the cross-sectional points θ studied and the influence of aligned wind and wave assumption
- The difference between the stiff and the flexible tower damage
- The variation in damage between the tower base, top and at height 60 meters

The fatigue damage is well below the criteria of design cumulative damage $D_D \leq 1$. The highest damage is about 0.34, which is considered low fatigue damage. Comparison to Erin E. Bachynski (2015) indicates that the fatigue damage should be higher, but the reference has different load cases, S-N curve and possibly tower properties, so a comparison is difficult. There are several possible explanations for the low damage. One interpretation is that the tower material is not utilized and could be less for a lifetime of 25 years. Another possibility could be that there are errors in the simulation or calculation of the fatigue. It is also possible that the design load cases and a limited number of wave seeds are not representative enough for the lifetime environment or that the percentage of each load case gives a non-conservative result. This will be looked further into in section 4.1.2.

As expected, the largest fatigue damage is at $\theta = 0°$ and $\theta = 180°$ due to a larger fore-aft bending moment than side-side bending moment. Small differences is seen between $\theta = 0°$ and $\theta = 180°$, and $\theta = 90°$ and $\theta = 270°$ due to the combined axial stress from axial force and bending moments in each point. The assumption of **aligned wind and waves** resulted in a very low side-side fatigue damage and it is probable that the damage is under predicted. A sensitivity study of the influence of misalignment on the structure is recommended to ensure that the analysis captures the entire lifetime damage.

As expected, the result show that the fatigue damage is **larger for the flexible tower** in points $\theta = 0°$ and $\theta = 180°$ which are strongly affected by the tower fore-aft bending moment. The exception is at the tower top, where the stiff tower experiences more fatigue damage. The tower top fore-aft bending moment for the stiff tower has larger stress ranges compared to the flexible tower, which can explain the larger fatigue damage value. The reason for a larger tower top fore-aft bending moment in the stiff model could be due to increased resistance against deflection.

In figure 4.1 it is seen that at angle $\theta = 0°$ and $\theta = 180°$, the largest damage is in the tower bottom as expected since the bending moments are largest here. For all directions, there is **large damage at tower height 60 meters**, and for $\theta = 90°$ and $\theta = 270°$ the damage is largest in this segment transition. The fatigue damage along the tower is affected by both the variation of cross-section properties and the load distribution along the tower. It is thus rational that the section at tower height 60 meters is taking up more load than the others. There is no significant change in diameter or thickness at this point compared to the others, so other reasons for the high fatigue damage will be explored.

At angle $\theta = 90°$ and $\theta = 270°$, the tower has **higher fatigue damage for the stiff model** along the length than for the flexible model. These points are most influenced by the side-side bending moment. This can indicate that the stiff model experience some resonance behaviour in these points. A spectral analysis is done to see if this is the case and displayed in figure 4.2b. It is seen that the stiff tower has power in the 3P area (0.3-0.48 Hz), which is most likely the reason for the larger fatigue damage compared to the flexible model. For a comparison, the spectral analysis is also done for the point at $\theta = 0°$ in figure 4.2a. At $\theta = 0°$ there is more energy content in the spectrum in total and in 1P and 3P areas. It is thus reasonable that this point experience more fatigue damage. The energy content could possibly be reduced by further calibration of the controller.

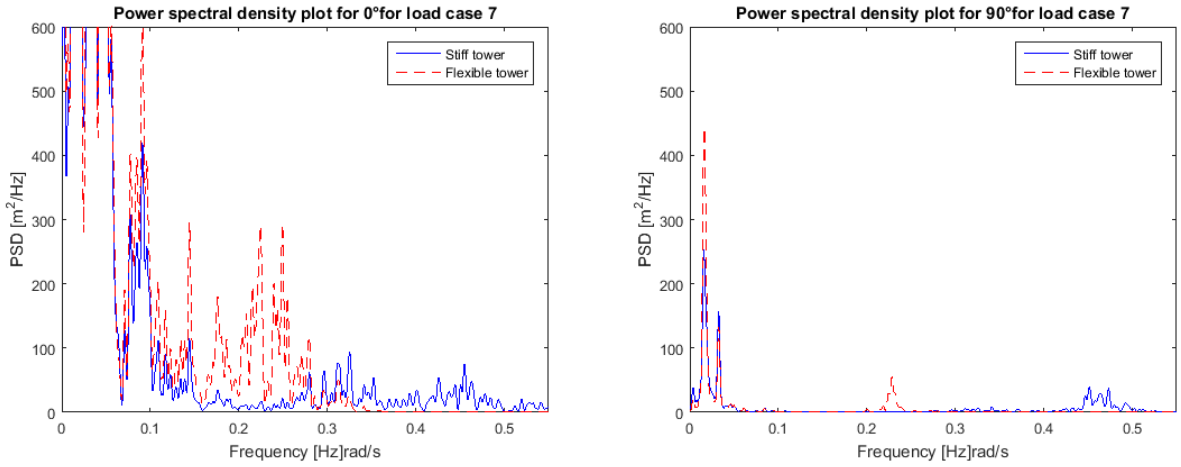

(a) 0° (b) 90°

Figure 4.2: Power spectral density vs. frequency for total stress in the tower at tower height 60 meters

The tower height at 60 meters experiences significantly fatigue damage and more than expected. The possible reasons for this will now be discussed. First, the **load distribution** is investigated as a possible reason. In figure 4.3, the standard deviation and mean to the forces, stresses and the combined axial stress from equation 3.6 is illustrated over the tower height. The axial force and bending moments are acting as expected with the largest mean and standard deviation in the bottom of the tower and decreasing with the height. The calculated stresses from the forces depend on the tower geometry. The figure shows that the stresses are acting differently than the forces due to the geometry changes. The fatigue damage has a similar shape as the standard deviation of the total stress, which is reasonable. The difference between the total stress standard deviation and mean is largest at the tower middle, which also can be an indication of larger fatigue damage here. The tower geometry's influence on the stress can thus be identified as a reason for the fatigue damage shape over the tower height.

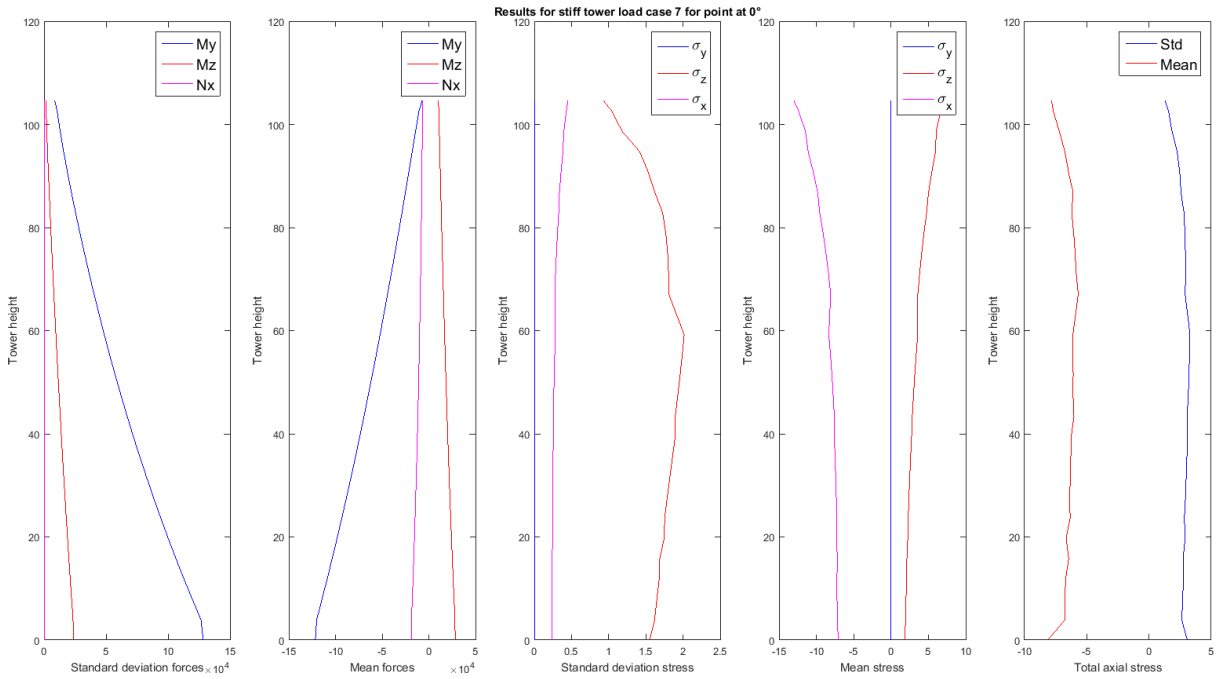

Figure 4.3: Standard deviation and mean of forces and stresses for stiff tower, load case 7 at 0°

Another possible reason for the large damage at tower height 60 meters could be the **mode shapes**. Figure 4.4 give the first fore-aft and side-side modes for the tower in red compared to the standstill in blue. A red horizontal line gives the location of the maximum fatigue damage. It is seen that in both cases the mode could be vibrating about the tower height 60 meters. This can be a reason for the larger fatigue damage at this point. The maximum curvature point of the mode shape can be subject to high fatigue damage, and from the plots it is possible that the maximum curvature is around the middle of the tower.

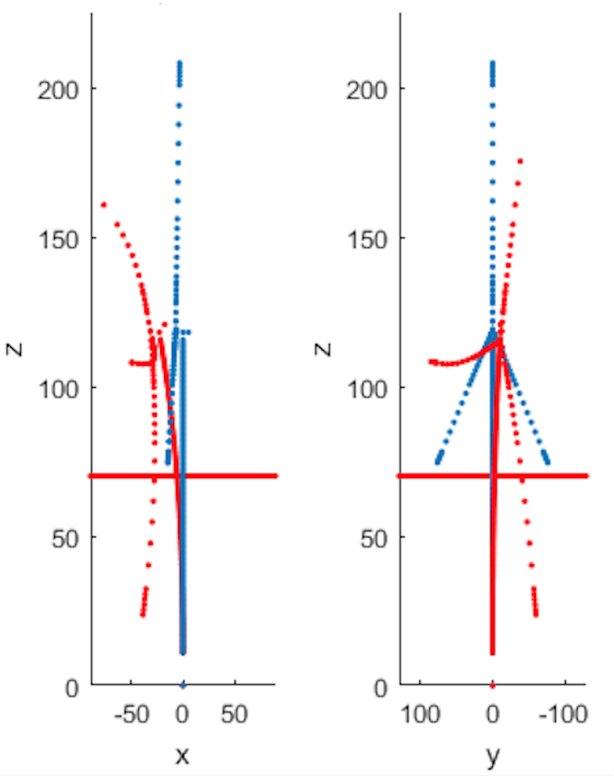

Figure 4.4: Mode shape 1st fore-aft and side-side tower mode, amplified with 1000 for illustration

The fatigue damage is well below the requirement and the results show that the cross-sectional properties and variation between the sections influence the damage. The largest damage is as expected in the tower base in the points most influenced by the fore-aft bending moments. The results are considered conservative due to the choices done in the methodology for the calculation. Because of the low total damage, there is a possibility that the material is not utilized and further optimization may be possible. This should be investigated further, and other sources of low damage are discussed in section 4.1.2.

4.1.2 Fatigue Damage per Condition

Figure 4.5 gives the damage per DLC for the tower base, top and at 60 meters. This figure shows the calculated 1-hour damage from each load case without accounting for the probability of occurrence. It is seen that load case 1 and 2 gives significantly small damage compared to the other load cases. This is because the first load cases are below rated wind speed and with mild wave climate. The fatigue damage is thus low because the applied loading is smaller. Load case 7 has the most severe wind and wave climate, and also represents the largest damage per hour.

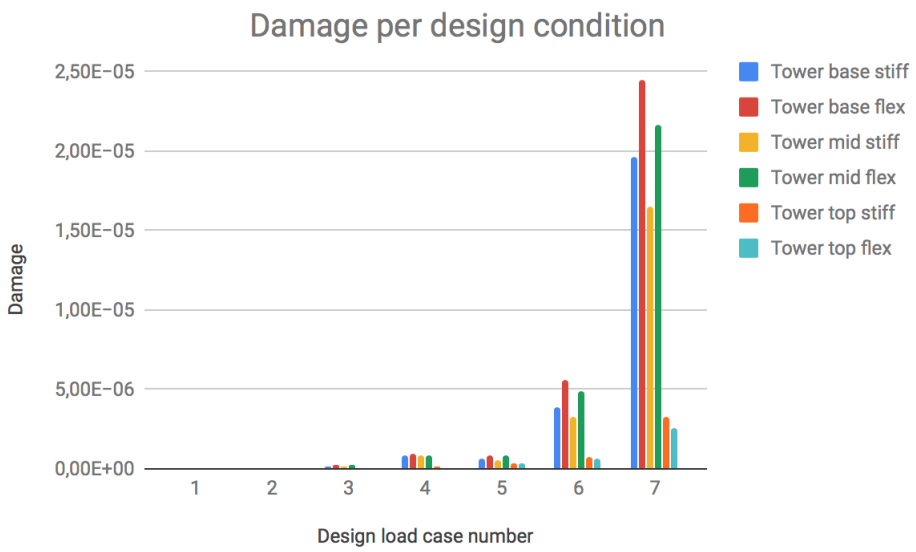

Figure 4.5: Total damage per condition in tower base, mid (60 m) and top at 0°without probability of occurrence

In the analysis done, 70% of the damage is from DLCs FLS2, FLS3 and FLS4. Figure 4.6 give the damage with the probability of occurrence for each load case. It is seen that DLC 2 give significantly small damage, and still represent 24% of the lifetime damage. This can be an explanation of the low fatigue damage. It is possible that more design load cases representing a larger variation of wind-wave climate would result in higher fatigue damage and give a more realistic representation. It is thus advised that further analysis will include more design load cases to see if this is the case.

Design load case 6 and 7 contribute significantly more than the others per hour, but due to a low probability of occurrence, their influence of the total damage is limited. Design load case 5 gives a lower contribution to the total damage than DLC 4, 6 and 7 for the tower base and at 60 meters. DLC 5 also has a lower damage per hour, seen in figure 4.5. The reason for this is difficult to state. DLC 5 has increased wind and wave loading compared to DLC 4 and is thus expected to have more fatigue damage per hour. The reason could have a correlation with the wave seeds, and thus the wave climate simulated. Further investigation should be to see if this is the explanation by including more wave seeds to ensure that the wave climate is represented correctly and that the effect is captured during the simulations.

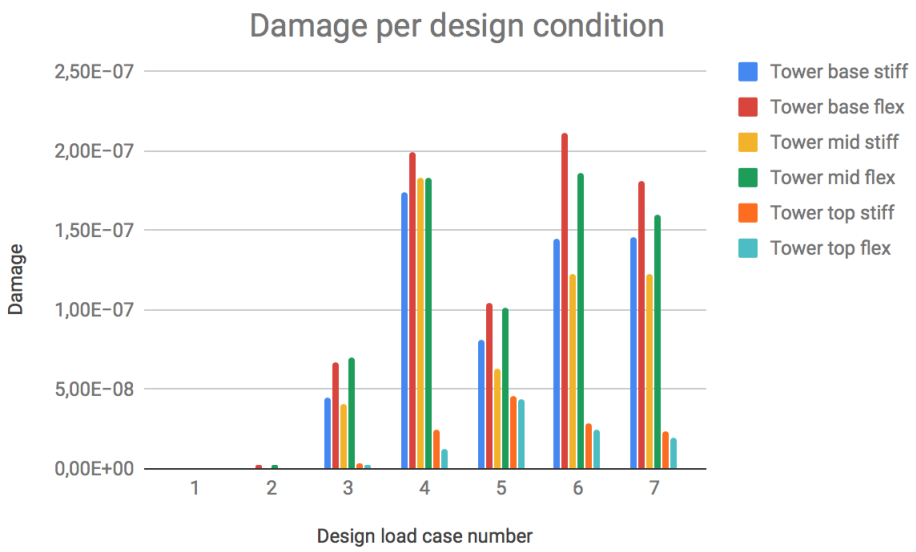

Figure 4.6: Total damage per condition in tower base, mid (60 m) and top at 0°with probability of occurrence

4.2 Results of the Spectral Analysis

A spectral analysis is done for the tower bending moments and the platform motions to identify resonance problems. Figure 4.7 give the power spectral density (PSD) for the bending moments in the tower bottom and segment at 60 meters tower height. Figure 4.7a give the fore-aft bending moment, and significant energy response is found below 0.01 Hz. There is also a resonance behaviour at a very low frequency. The PSD is associated with the wind spectrum and could possibly also be amplified by the wave energy. No energy is observed above 0.1 Hz, so the 1P and 3P regions do not affect the bending moments PSD. The flexible tower has a larger amplification of the bending moments compared to the stiff tower at the largest amplification frequencies. It is seen that the amplification is higher at the tower base compared to at tower height 60 meters, as expected for the bending moments.

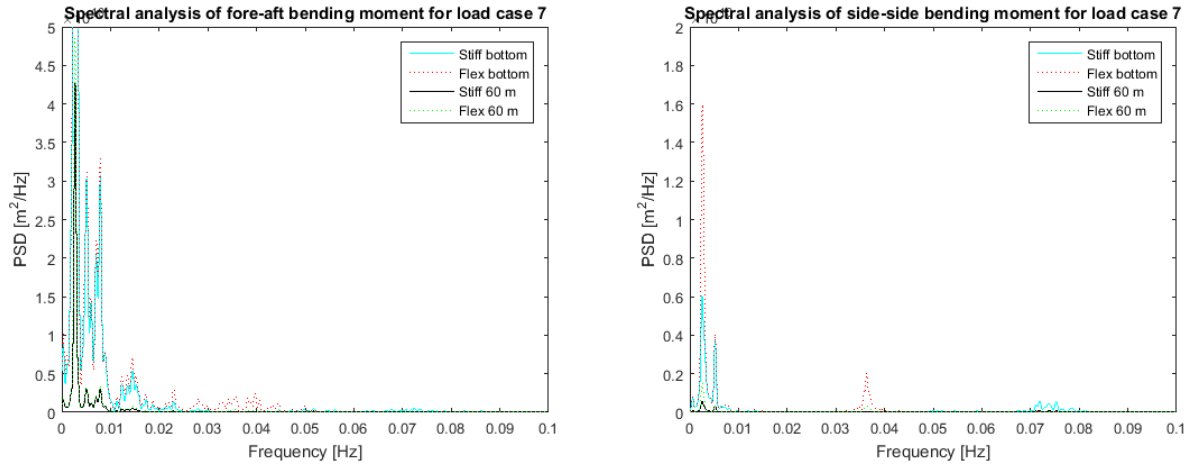

(a) Fore-aft bending moment

(b) Side-side bending moment

Figure 4.7: Power spectral density vs. frequency for tower base bending moment

A spectral analysis is done for each of the six platform motions. The figures are scaled to show the maximum PSD and have a frequency limit of 0.15 Hz since there is no energy distribution is above this frequency. The analysis is done for design load case FLS7 to see the influence of severe wind and wave climate. Figure 4.8 give the spectral plots. All motions have its resonant response with the largest amplification at its natural frequency, as expected. The results compare well to the results in DTU (2018). The linked surge-sway and roll-pitch motions give similar spectres due to symmetry of the platform. In the free decay tests done to identify the platform frequencies, small differences were found between the models with a stiff and flexible tower. The small differences can be observed in figure 4.8 for the models. However, very limited differences are seen for maximum amplification in the plots, but the trend of which model has a slightly higher natural frequency is consistent with the decay tests.

The surge motion has energy content in the low-frequency turbulent wind frequency, and some in the range 0.05-0.1 Hz which is likely to be from wave frequency response. This is as expected by the surge motion and corresponds well to Cheng et al. (2017). The roll, pitch and yaw motions show a response at the wind spectrum frequency, which is natural when the turbulent wind is applied to the model. The roll and pitch spectrum has a response around 0.05 Hz, corresponding to the heave natural frequency and possibly also influenced by wave response.

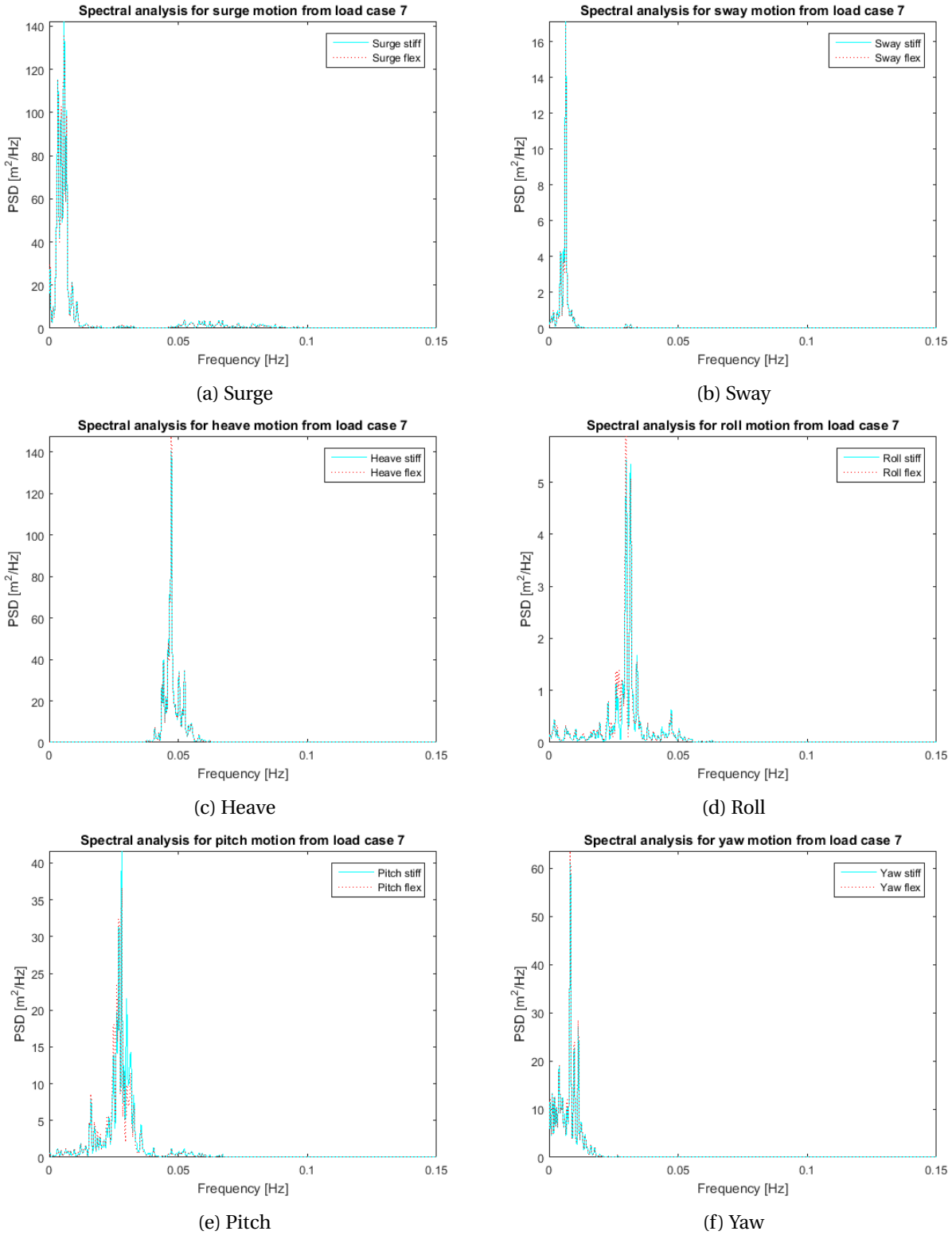

(a) Surge

(b) Sway

(c) Heave

(d) Roll

(e) Pitch

(f) Yaw

Figure 4.8: Power spectral density vs. frequency for platform motions

4.3 Ultimate Limit State Assessment

This section will examine the significance of extreme load cases. Fatigue is said to be a crucial limit state for a wind turbine design, but with a flexible tower the ultimate limit state can become decisive for the design.

4.3.1 Ultimate Strength Analysis

Table 4.1 gives the result from the yield check. The maximum von Mises stress was found for each load case and checked with the material factor γ_m against the yield strength 355 MPa. The von Mises stress is found from the tower base, tower top or tower middle, and the maximum value is chosen. It is seen that all design load cases for both the stiff and the flexible tower are well below the yield limit of 355 MPa. The flexible tower has a higher von Mises stress compared to the stiff tower for DLC ULS1 and ULS2 when the turbine is operating. When the turbine is parked in DLC ULS3, the flexible tower experiences a lower maximum von Mises stress. The reason for this could be that the stiff tower will resist deflection and rotation more than the flexible tower, so the stresses become higher. The flexible tower will allow more deflection and thus experience slightly lower stress. When the wind turbine is in operating condition, the stresses are higher in the flexible tower. In operating condition, there are many aspects that affect the stress in the tower, and the trend show that the flexible tower experiences more von Mises stress than the stiff.

DLC	Stiff-stiff ULS 1	Stiff-stiff ULS 2	Stiff-stiff ULS 3	Soft-stiff ULS 1	Soft-stiff ULS 2	Soft-stiff ULS 3
Max von Mises stress [MPa]	96.03	99	107	100.9	113.9	105.7
$\sigma_{vonMises} \cdot \gamma_m$ [MPa]	110.4345	113.8500	123.0500	116.0350	130.9850	121.5550

Table 4.1: Yield check results for each design load case for ULS

The flexible tower has an elasticity modulus one quarter lower than the stiff tower. This can not represent a real material, and the yield strength is thus assumed to be the same. If the yield strength were also lowered to one quarter, it would be 88.75 MPa and the yield strength would have been exceeded. This is not a realistic situation since a material like this would lead to fracture. It is however advised that a yield

check is also done for a realistic flexible tower to ensure sufficient strength against yield failure.

4.3.2 Buckling Check

The buckling check is done by calculating η and check if it is below $\eta_{allowed} = \frac{1}{\gamma_m} = 0.8696$. The tower is simplified to have a constant cross-section along the length. The dimensions for the tower bottom, tower top and tower middle at segment 13 are checked. Table 4.2 give the calculated η for each load case and cross-section dimensions.

DLC / η	Stiff-stiff ULS 1	Stiff-stiff ULS 2	Stiff-stiff ULS 3	Soft-stiff ULS 1	Soft-stiff ULS 2	Soft-stiff ULS 3
Tower bottom	0.0056	0.0062	0.0049	0.0073	0.0084	0.0067
Tower middle	0.0464	0.0511	0.0406	0.0744	0.0846	0.0705
Tower top	0.0767	0.0852	0.0863	0.2274	0.2352	0.2335

Table 4.2: Buckling check results for each design load case for ULS

All results from the buckling calculation are well below the criteria and the tower is considered safe from buckling failure. The largest η for both the stiff and flexible tower is with tower top properties. This is as expected since the tower top properties give the largest slenderness ratio. The stiff tower has lower η values than the flexible tower for the same load case and tower cross-section. This is because of the lower elasticity modulus for the flexible tower. The results show that a buckling check becomes more important for a flexible tower and that the slenderness ratio has a large impact on the buckling analysis. This indicates that the ultimate limit state can become decisive for the design of a flexible tower since the slenderness ratio must be kept within safe limits.

4.3.3 Blade-tip to Tower Clearance

The blade tip clearance to the tower is illustrated in figure 4.9. Here, the tower max deflection is used for each point along the tower height. The blade tip deflection is the maximum value during the simulation

for the flexible tower from DLC ULS2 as this gave the largest blade deflection. The blades are deflected more in the operational state than in the parked condition, as expected. It is seen that the blade tip does not cross the criteria of 13.64 meters distance. This is a simplified analysis where the influence of rotation and deflection of the tower on the angle of the blades are not accounted for. The criteria curve follow the tower deflection so a constant value of 13.64 meters is held.

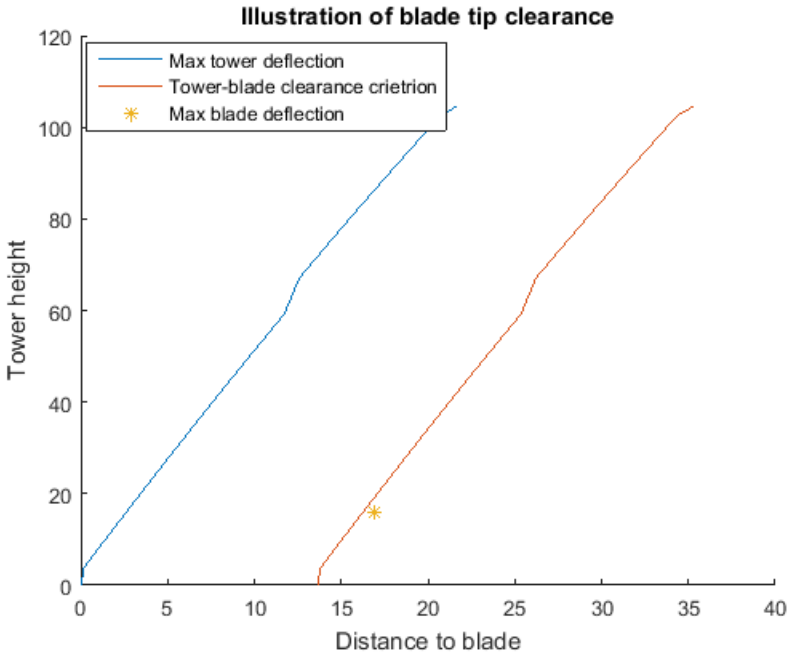

Figure 4.9: Blade tip clearance for flexible tower for DLC ULS2

The analysis method used proved to be difficult to thrust. In addition to deflections, rotations should be accounted for to ensure a safe design. It is also difficult to interpret the output from SIMA for the tower and blades simultaneously. The tower deflection depends on the movements of the platform and it is difficult to see when the blades pass in front of the tower. Improvements of the analysis method are recommended for further work to ensure a sufficient distance is maintained. The further work should include rotations of the tower and the influence this has on the angle of the blades to the tower. In addition, it would be interesting to see how the tower and blades move in comparison to each other under the maximum loads from the design load case.

Chapter 5

Conclusion and Recommendations for Further Work

5.1 Conclusion

A comparison of a stiff-stiff and a soft-stiff tower was done to examine the possibility of introducing a flexible tower to the floating wind turbine concept OO-Star Wind Floater. The investigation was based on time-domain analysis for fatigue and ultimate limit state design.

The results from the fatigue analysis gave a safe design for both tower models during a lifetime of 25 years. The flexible tower was exposed to more fatigue damage in the points exposed to the fore-aft bending moment, and less than the stiff tower in the points exposed to side-side bending moment. The reason for this was identified to be due to 3P amplification of the side-side natural frequency for the stiff model. The fatigue damage was largest in the tower bottom, as expected due to the tower bottom experiencing the largest bending moments. There was also large damage at tower height 60 meters. The reason for this was identified to be a combination of cross-section variations, mode shape and load distribution along the tower.

A spectral analysis was used to investigate resonance behaviour. There were no indications of resonance induced by the wind turbine rotational frequencies for the platform motions or tower base bending moments. The bending moments and total stress have power in the rotational frequency and blade passing frequency ranges. The stiff tower has most power in the 3P area, while the flexible tower has power in the

1P range. This could possibly be decreased by further calibration of the controller. Since both models are safe from fatigue damage during the lifetime, this is not considered to be critical for the safety of the structure.

The ultimate limit state analysis was used to check the design against yield failure, buckling and blade-tip to tower interaction. The yield and buckling failure were difficult to examine because of the method used to make the tower flexible. Since the flexible tower model was made with an unreal elasticity modulus, the results were difficult to use to validate the flexible tower behaviour under extreme loading. The goal was to see if ultimate limit design became determining for the design of the flexible tower, as fatigue is considered to be the decisive parameter for the tower design. The yield check was within the limits, and the higher stress for the flexible tower compared to the stiff did not indicate yield failure in a realistic model. However, due to the difficulty with reasoning the results, it is advised to also do the yield check for a realistic model to ensure a safe design. The buckling check showed that both models are well below the criteria. Buckling failure could become decisive for the design unless the slenderness ratio of the cross-sections is limited. The maximum blade-tip deflection towards the tower did not cross the limit of safe clearance. The method used for finding the clearance was not considered sufficient to justify the results, and a further analysis was advised.

Based on the results, a flexible tower is considered safe to include in the OO-Star wind Floater concept. This thesis has only researched the possibility of having a flexible tower and a realistic tower design must be made. It is advised that the flexible tower design is found by varying the wall thickness and diameter to a first tower natural frequency in the soft-stiff frequency range.

5.2 Recommendations for Further Work

Further work is highly recommended on this topic. This thesis proved that the OO-Star Wind Floater is capable of having a soft-stiff tower. Further work is recommended as follows:

1. A realistic flexible tower model should be made. It is recommended to vary the wall thickness and the diameter to find a design with a soft-stiff first tower natural frequency. The thickness and diameter change should be within recommended diameter to thickness ratio and diameter to length ratio from the standards.

2. Several more design load cases with at least three variations of wave seeds are recommended to

use in the fatigue assessment to ensure a correct caption of the loading and responses during the lifetime of the structure.

3. A sensitivity analysis for the wind and wave misalignment is recommended to check the under and over prediction of fatigue damage in side-side and fore-aft direction, respectively.

4. An ultimate strength analysis should be done to ensure that the structure is safe from yield failure. This could be done for an operating wind turbine with severe wind and wave climate to capture the maximum von Mises stress.

5. A buckling check should be done if the slenderness ratio of the tower is much higher than conventional towers. If hand calculations show danger of buckling failure, an analysis in software should be used to ensure a safe design.

6. The blade-tip clearance to the tower should be investigated further in a better analysis to ensure that a safe distance is maintained. This analysis should account for tower and blade deflections and rotations.

7. Further calibration of the wind turbine controller can reduce the tower response found due to the rotational frequencies.

Bibliography

Arany, L., Bhattacharya, S., Macdonald, J. H., and Hogan, S. J. (2016). Closed form solution of eigen frequency of monopile supported offshore wind turbines in deeper waters incorporating stiffness of substructure and ssi. *Soil Dynamics and Earthquake Engineering*, 83:18 – 32.

Bachynski, E. (2018). Lecture notes in course integrated dynamic analysis of wind turbines.

Bachynski, E., Kvittem, M. I., Luan, C., and Moan, T. (2014). Wind-wave misalignment effects on floating wind turbines: Motions and tower load effects. *Journal of Offshore Mechanics and Arctic Engineering*, 136:041902.

Bhattacharya, S. (2014). Challenges in design of foundations for offshore wind turbines. *The Institution of Engineering and Technology*.

Bhattacharya, S., Arany, L., macdonald, J., and Hogan, S. (2014). 2014 wind energy online. *W*.

Brodtkorb, P., Johannesson, P., Lindgren, G., Rychlik, I., Rydén, J., and Sjö, E. (2000). WAFO - a Matlab toolbox for the analysis of random waves and loads. In *Proc. 10'th Int. Offshore and Polar Eng. Conf., ISOPE, Seattle, USA*, volume 3, pages 343–350.

Burton, T., J. N. S. D. B. E. (2011). *Wind Energy Handbook*. John Wiley & Sons.

Butterfield, S., Musial, W., Jonkman, J., and Sclavounos, P. (Sat Sep 01 00:00:00 EDT 2007). Engineering challenges for floating offshore wind turbines. *NREL*.

Cheng, Z., Madsen, H. A., Gao, Z., and Moan, T. (2017). Effect of the number of blades on the dynamics of floating straight-bladed vertical axis wind turbines. *Renewable Energy*, 101:1285 – 1298.

Christian Bak, Frederik Zahle, R. B. T. K. A. Y. L. C. H. A. N.-M. H. (2013a). Description of the dtu 10 mw reference wind turbine. Technical report, DTU Wind Energy.

Christian Bak, Frederik Zahle, R. B. T. K. A. Y. L. C. H. A. N.-r. M. H. H. (2013b). Description of the dtu 10 mw reference wind turbine. Technical Report DTU Wind Energy Report-I-0092, DTU Wind Energy.

Community, S. P. (2018). Natural frequency and resonance. https://community.plm.automation.siemens.com/t5/Testing-Knowledge-Base/Natural-Frequency-and-Resonance/ta-p/498422.

DNV (2010). *DNV-OS-J103 Design of Floating Wind Turbine Structures*.

DNV (2014). *DNV-OS-J101 Design of Offshore Wind Turbine Structures*.

DNV (2016a). *DNVGL-ST-0126 Support structures for wind turbines*.

DNV (2016b). *DNVGL-ST-0437 Loads and site conditions for wind turbines*.

DNVGL (2015). Deliverable d7.2 design basis. Technical report, Lifes50+.

Dong-young Kim, Joongho Lee, Ji-Hyung Park, and JungHyun Han (2011). Wave seeds. In *2011 IEEE International Conference on Multimedia and Expo*, pages 1–4.

DTU (2015). Deliverable d1.2 wind turbine models for the design. Technical report, DTU, LIFES50+.

DTU (2018). Deliverable d4.5 state-of-the-art models for the two lifes50+ 10mw floater concepts. Technical report, Lifes50+.

Duan, F. (2017). Wind energy cost analysis - coe for offshore wind and lcoe financial modeling. Master's thesis, Helsinki Metropolia University of Applied Sciences.

Erin E. Bachynski, H. O. (2015). Hydrodynamic modeling of large-diameter bottom-fixed offshorewind turbines. In *OMAE2015-42028*.

Haritos, N. (2019). Modelling ocean waves and their effects on offshore structures. -.

Hau, E. (2013). *Wind Turbines*. Springer Berlin Heidelberg, Berlin, Heidelberg.

Horcas, S. G., Debrabandere, F., Tartinville, B., Hirsch, C., and Coussement, G. (2016). *CFD Study of DTU 10 MW RWT Aeroelasticity and Rotor-Tower Interactions*, pages 309–334. Springer International Publishing, Cham.

Huhn, Martin & Hopp, M. . J. C. (2015). Additional design criteria for wind turbines: Excitation to mechanical vibrations from the power system. *VDI-Fachtagung Schwingungen von Windenergieanlagen*, 6(2242).

Jay, A., Myers, A. T., Torabian, S., Mahmoud, A., Smith, E., Agbayani, N., and Schafer, B. W. (2016). Spirally welded steel wind towers: Buckling experiments, analyses, and research needs. *Journal of Constructional Steel Research*, 125:218 – 226.

Jiang, Z., Zhu, X., and Hu, W. (2018). *Modeling and Analysis of Offshore Floating Wind Turbines*, pages 247–280. Springer International Publishing, Cham.

Kvittem, M. I. and Moan, T. (2015). Time domain analysis procedures for fatigue assessment of a semi-submersible wind turbine. *Marine Structures*.

L. Barj, Susan Stewart, G. S. M. L. J. J. A. R. (2014). Wind/wave misalignment in the loads analysis of a floating offshore wind turbine. In *NREL/CP-5000-61043*.

Landbø, T. (2018). Oo-star wind floater the future of offshore wind? https://www.sintef.no/globalassets/project/eera-deepwind-2018/presentations/closing$_l andbo.pdf$.

Li, Q., Gao, Z., and Moan, T. (2017). Modified environmental contour method to determine the long-term extreme responses of a semi-submersible wind turbine. *Ocean Engineering*, 142:563 – 576.

Licari, J., Ekanayake, J. B., and Jenkins, N. (2013). Investigation of a speed exclusion zone to prevent tower resonance in variable-speed wind turbines. *IEEE Transactions on Sustainable Energy*, 4(4):977–984.

Luan, C. (2018). Design and analysis for a steel braceless semi-submersible hull for supporting a 5-mw horizontal axis wind turbine.

M Jonkman, J. and J Jonkman, B. (2016). Fast modularization framework for wind turbine simulation: full-system linearization. *Journal of Physics: Conference Series*, 753:082010.

MathWorks (2019). Practical introduction to frequency-domain analysis. https://se.mathworks.com/help/signal/examples/practical-introduction-to-frequency-domain-analysis.html.

Miceli, F. (2017). Type of towers – stiff, soft or soft soft? http://www.windfarmbop.com/type-of-towers-stiff-soft-or-soft-soft/.

Mikel [Iribas, Morten H. Hansen, M. M. C. T. A. N. E. B. A. S.-P. J. W. L. D. S. (2017). Deliverable report d1.42 - methodology for feed-forward control strategies using nacelle or blade based sensors and distributed control. Technical report, Innwind, DTU.

of Stuttgart, U. (2018). Deliverable d4.2 public definition of the two lifes50+ 10mw floater concepts. Technical report, DTU, LIFES50+.

Pablo Gomez, Gustavo Sanchez, A. L. G. G. (2015). Deliverable 1.1 oceanographic and meteorological conditions for the design. Technical report, Lifes50+.

SINTEF. Sima. https://www.sintef.no/en/software/sima/.

Sirnivas, S., Musial, W., Bailey, B., and Filippelli, M. (2014). Assessment of offshore wind system design, safety, and operation standards.

Stavridou, N., Efthymiou, E., and Baniotopoulos, C. (2015). Welded connections of wind turbine towers under fatigue loading: Finite element analysis and comparative study. *American Journal of Engineering and Applied Sciences*, 8:489–503.

Tecnalia (2017). Deliverable d1.6 upscaling procedures. Technical report, Lifes50+.

USTUTT (2016). D 7.4 state-of-the-art fowt design practice and guidelines. Technical report, Lifes50+.

Wikipedia (2019). First principle. https://en.wikipedia.org/wiki/First$_p rinciple$.

Xue, W. (2016). Design, numerical modelling and analysis of a spar floater supporting the dtu 10mw wind turbine. Master's thesis, Norwegian University of Science and Technology.

Appendices

A Controller files

A1 Controller input

```
1  10000.0                    ;Rated power [kW]
2  0.6283                     ;Minimum rotor speed [rad/s]
3  1.005                      ;Rated rotor speed [rad/s]
4  15.6E+07                   ;Maximum allowable generator torque [Nm]
5  100.0                      ;Minimum pitch angle, theta_min [deg], if |
       theta_min|>90, then a table of <wsp,theta_min> is read from a file named '
       wptable.n', where n=int(theta_min)
6  82.0                       ;Maximum pitch angle [deg]
7  10.0                       ;Maximum pitch velocity operation [deg/s]
8  0.4                        ;Frequency of generator speed filter [Hz]
9  0.7                        ;Damping ratio of speed filter [-]
10 3.43                       ;Frequency of free-free DT torsion mode [Hz], if
       zero no notch filter used, Partial load control parameters
11 13013100.0                 ;Optimal Cp tracking K factor [Nm/(rad/s)^2], Qg=
       K*Omega^2, K=eta*0.5*rho*A*Cp_opt*R^3/lambda_opt^3
12 0.683456E+08               ;Proportional gain of torque controller [Nm/(rad/
       s)]
13 0.153367E+08               ;Integral gain of torque controller [Nm/rad]
14 0.0                        ;Differential gain of torque controller [Nm/(rad/
       s^2)] Full load control parameters
15 2                          ;Generator control switch [1=constant power, 2=
       constant torque]
16 1.922009003E-01            ;Proportional gain of pitch controller [rad/(rad/
       s)]
17 8.798198990E-03            ;Integral gain of pitch controller [rad/rad]
18 0.0                        ;Differential gain of pitch controller [rad/(rad/
       s^2)]
19 0.4e-8                     ;Proportional power error gain [rad/W]
```

```
20 0.4e-8                    ;Integral power error gain [rad/(Ws)]
21 198.32888                 ;Coefficient of linear term in aerodynamic gain
   scheduling, KK1 [deg]
22 693.22213                 ;Coefficient of quadratic term in aerodynamic
   gain scheduling, KK2 [deg^2] & (if zero, KK1 = pitch angle at double gain)
23 1.3                       ;Relative speed for double nonlinear gain [-] Cut
   -in simulation parameters
24 2.0                       ;Cut-in time [s]
25 1.0                       ;Time delay for soft start of torque [1/1P] Cut-
   out simulation parameters
26 -1                        ;Cut-out time [s]
27 5.0                       ;Time constant for linear torque cut-out [s]
28 1                         ;Stop type [1=normal, 2=emergency]
29 1.0                       ;Time delay for pitch stop after shut-down signal
    [s]
30 3                         ;Maximum pitch velocity during initial period of
   stop [deg/s]
31 3.0                       ;Time period of initial pitch stop phase [s] (
   maintains pitch speed specified in constant 30)
32 4                         ;Maximum pitch velocity during final phase of
   stop [deg/s] Expert parameters (keep default values unless otherwise given)
33 2.0                       ;Lower angle above lowest minimum pitch angle for
    switch [deg]
34 2.0                       ;Upper angle above lowest minimum pitch angle for
    switch [deg], if equal then hard switch
35 95.0                      ;Ratio between filtered speed and reference speed
    for fully open torque limits [%]
36 2.0                       ;Time constant of 1st order filter on wind speed
   used for minimum pitch [1/1P]
37 1.0                       ;Time constant of 1st order filter on pitch angle
    used for gain scheduling [1/1P] Drivetrain damper
38 0.0                       ;Proportional gain of active DT damper [Nm/(rad/s
```

```
)], requires frequency in input 10 Over speed
39 100.0                    ;Overspeed percentage before initiating turbine
   controller alarm (shut-down) [%] Additional non-linear pitch control term (not
    used when all zero)
40 0.0                      ;Err0 [rad/s]
41 0.0                      ;ErrDot0 [rad/s^2]
42 0.0                      ;PitNonLin1 [rad/s] Storm control command
43 28.0                     ;Wind speed 'Vstorm' above which derating of
   rotor speed is used [m/s]
44 28.0                     ;Cut-out wind speed (only used for derating of
   rotor speed in storm) [m/s] Safety system parameters
45 100.0                    ;Overspeed percentage before initiating safety
   system alarm (shut-down) [%]
46 10.5                     ;Max low-pass filtered tower top acceleration
   level [m/s^2] - max in DLC 1.3=1.1 m/s^2    Turbine parameter
47 178.0                    ;Nominal rotor diameter [m] Parameters for rotor
   inertia reduction in variable speed region
48 0.0                      ;Proportional gain on rotor acceleration in
   variable speed region [Nm/(rad/s^2)] (not used when zero)    Parameters for
   alternative partial load controller with PI regulated TSR tracking
49 7.8                      ;Optimal tip speed ratio [-] (only used when K=
   constant 11 = 0 otherwise  Qg=K*Omega^2 is used)    Parameters for adding
   aerodynamic drivetrain damping on gain scheduling
50 0.0                      ;Proportional gain of aerodynamic DT damping [Nm
   /(rad/s)]
51 0.0                      ;Coefficient of linear term in aerodynamic DT
   damping scheduling, KK1 [deg]
52 0.0                      ;Coefficient of quadratic term in aerodynamic DT
   damping scheduling, KK2 [deg^2]  Torque exclusion zone
53 10                       ;Torque exclusion zone: Low speed [rad/s] = 5.5
   5.9 rpm
54 6.634e6                  ;Torque exclusion zone: Low speed generator toque
```

[Nm]

55 20 ;Torque exclusion zone: High speed [rad/s] = 6.5 6.1 rpm

56 4.438e6 ;Torque exclusion zone: High speed generator toque [Nm]

57 25 ;Time constant of reference switching at exclusion zone [s] 1st DT torsion mode damper

58 1.77 ;Frequency of notch filter [Hz]

59 0.2 ;Damping of BP filter [-]

60 0.01 ;Damping of notch filter [-]

61 0.1 ;Phase lag of damper [s] => max 40*dt Fore-aft Tower mode damper

62 0.30 ;Frequency of BP filter [Hz]

63 0.47 ;Frequency of notch fiter [Hz]

64 0.02 ;Damping of BP filter [-]

65 0.01 ;Damping of notch filter [-]

66 2e-2 ;Gain of damper [-]

67 0.3 ;Phase lag of damper [s] => max 40*dt

68 0.18 ;Time constant of 1st order filter on PWR used for fore-aft Tower mode damper GS [Hz]

69 0.5 ;Lower PWR limit used for fore-aft Tower mode damper GS [-]

70 0.8 ;Upper PWR limit used for fore-aft Tower mode damper GS [-] Side-to-side Tower mode filter

71 0.256 ;Frequency of Tower side-to-side notch filter [Hz]

72 0.01 ;Damping of notch filter [-] Safety system parameters

73 10.1 ;Max low-pass filtered tower top acceleration level before initiating safety system alarm (shut-down) [m/s^2]

74 1 ;

75 1 ;

```
76 1                                    ;Gear ratio
```

A2 Pitch table

8 Wind speed [m/s]	Pitch [deg]
4.000000	2.893113
5.000000	2.122761
6.000000	1.086778
7.000000	0.000078
8.000000	0.000018
9.000000	0.000078
10.000000	0.000018
25.000000	0.000018

B TurbSim input file

```
1  TurbSim Input File. Valid for TurbSim v1.50, 25-Sep-2009; Input File for
       Certification Test #3 (Kaimal Spectrum, formatted FF files).
2
3  ---------Runtime Options-----------------------------------
4  -382116359          RandSeed1       - First random seed  (-2147483648 to
       2147483647)
5  740207055           RandSeed2       - Second random seed (-2147483648 to
       2147483647) for intrinsic pRNG, or an alternative pRNG: "RanLux" or "RNSNLW"
6  False               WrBHHTP         - Output hub-height turbulence parameters in
       GenPro-binary form?  (Generates RootName.bin)
7  False               WrFHHTP         - Output hub-height turbulence parameters in
       formatted form?  (Generates RootName.dat)
8  False               WrADHH          - Output hub-height time-series data in AeroDyn
       form?  (Generates RootName.hh)
9  False               WrADFF          - Output full-field time-series data in TurbSim/
       AeroDyn form? (Generates RootName.bts)
10 True                WrBLFF          - Output full-field time-series data in BLADED/
       AeroDyn form?  (Generates RootName.wnd)
11 False               WrADTWR         - Output tower time-series data? (Generates
       RootName.twr)
12 False               WrFMTFF         - Output full-field time-series data in
       formatted (readable) form?  (Generates RootName.u, RootName.v, RootName.w)
13 False               WrACT           - Output coherent turbulence time steps in
       AeroDyn form? (Generates RootName.cts)
14 True                Clockwise       - Clockwise rotation looking downwind? (used
       only for full-field binary files - not necessary for AeroDyn)
15  0                  ScaleIEC        - Scale IEC turbulence models to exact target
       standard deviation? [0=no additional scaling; 1=use hub scale uniformly; 2=
       use individual scales]
16
```

```
17 --------Turbine/Model Specifications-----------------------
18 32                NumGrid_Z       - Vertical grid-point matrix dimension
19 32                NumGrid_Y       - Horizontal grid-point matrix dimension
20 0.05              TimeStep        - Time step [seconds]
21 3600.0            AnalysisTime    - Length of analysis time series [seconds] (
       program will add time if necessary: AnalysisTime = MAX(AnalysisTime,
       UsableTime+GridWidth/MeanHHWS) )
22 3600.0            UsableTime      - Usable length of output time series [seconds
       ] (program will add GridWidth/MeanHHWS seconds)
23 119.00            HubHt           - Hub height [m] (should be > 0.5*GridHeight)
24 200.00            GridHeight      - Grid height [m]
25 200.00            GridWidth       - Grid width [m] (should be >= 2*(RotorRadius+
       ShaftLength))
26 0                 VFlowAng        - Vertical mean flow (uptilt) angle [degrees]
27 0                 HFlowAng        - Horizontal mean flow (skew) angle [degrees]
28
29 --------Meteorological Boundary Conditions-------------------
30 "IECKAI"          TurbModel       - Turbulence model ("IECKAI"=Kaimal, "IECVKM"=
       von Karman, "GP_LLJ", "NWTCUP", "SMOOTH", "WF_UPW", "WF_07D", "WF_14D", or "
       NONE")
31 "3"               IECstandard     - Number of IEC 61400-x standard (x=1,2, or 3
       with optional 61400-1 edition number (i.e. "1-Ed2") )
32 "C"               IECturbc        - IEC turbulence characteristic ("A", "B", "C"
       or the turbulence intensity in percent) ("KHTEST" option with NWTCUP, not used
        for other models)
33 "NTM"             IEC_WindType    - IEC turbulence type ("NTM"=normal, "xETM"=
       extreme turbulence, "xEWM1"=extreme 1-year wind, "xEWM50"=extreme 50-year wind
       , where x=wind turbine class 1, 2, or 3)
34 default           ETMc            - IEC ETM "c" parameter [m/s] (or "default")
35 "PL"              WindProfileType - Wind profile type ("JET"=Low-level jet,"LOG"=
       Logarithmic,"PL"=Power law, or "default")
36 119.00            RefHt           - Height of the reference wind speed [m]
```

```
5                   URef            - Mean (total) wind speed at the reference height [m/s]
350                 ZJetMax         - Jet height [m] (used only for JET wind profile, valid 70-490 m)
0.14                PLExp           - Power law exponent  (or "default")
0.0003              Z0              - Surface roughness length [m] (or "default")

--------Non-IEC Meteorological Boundary Conditions------------
default             Latitude        - Site latitude [degrees] (or "default")
0.05                RICH_NO         - Gradient Richardson number
default             UStar           - Friction or shear velocity [m/s] (or "default")
default             ZI              - Mixing layer depth [m] (or "default")
default             PC_UW           - Mean hub u'w' Reynolds stress (or "default" or "none")
default             PC_UV           - Mean hub u'v' Reynolds stress (or "default" or "none")
default             PC_VW           - Mean hub v'w' Reynolds stress (or "default" or "none")
default             IncDec1         - u-component coherence parameters (e.g. "10.0 0.3e-3" in quotes) (or "default")
default             IncDec2         - v-component coherence parameters (e.g. "10.0 0.3e-3" in quotes) (or "default")
default             IncDec3         - w-component coherence parameters (e.g. "10.0 0.3e-3" in quotes) (or "default")
default             CohExp          - Coherence exponent (or "default")

--------Coherent Turbulence Scaling Parameters-------------------
".\EventData"       CTEventPath     - Name of the path where event data files are located
random              CTEventFile     - Type of event files ("random", "les" or "dns")
true                Randomize       - Randomize disturbance scale and location? (
```

```
      true/false)
59    1.0             DistScl         - Disturbance scale (ratio of dataset height to
          rotor disk).
60    0.5             CTLy            - Fractional location of tower centerline from
          right (looking downwind) to left side of the dataset.
61    0.5             CTLz            - Fractional location of hub height from the
          bottom of the dataset.
62    30.0            CTStartTime     - Minimum start time for coherent structures in
          RootName.cts [seconds]
63
64    ================================================
65    NOTE: Do not add or remove any lines in this file!
66    ================================================
```

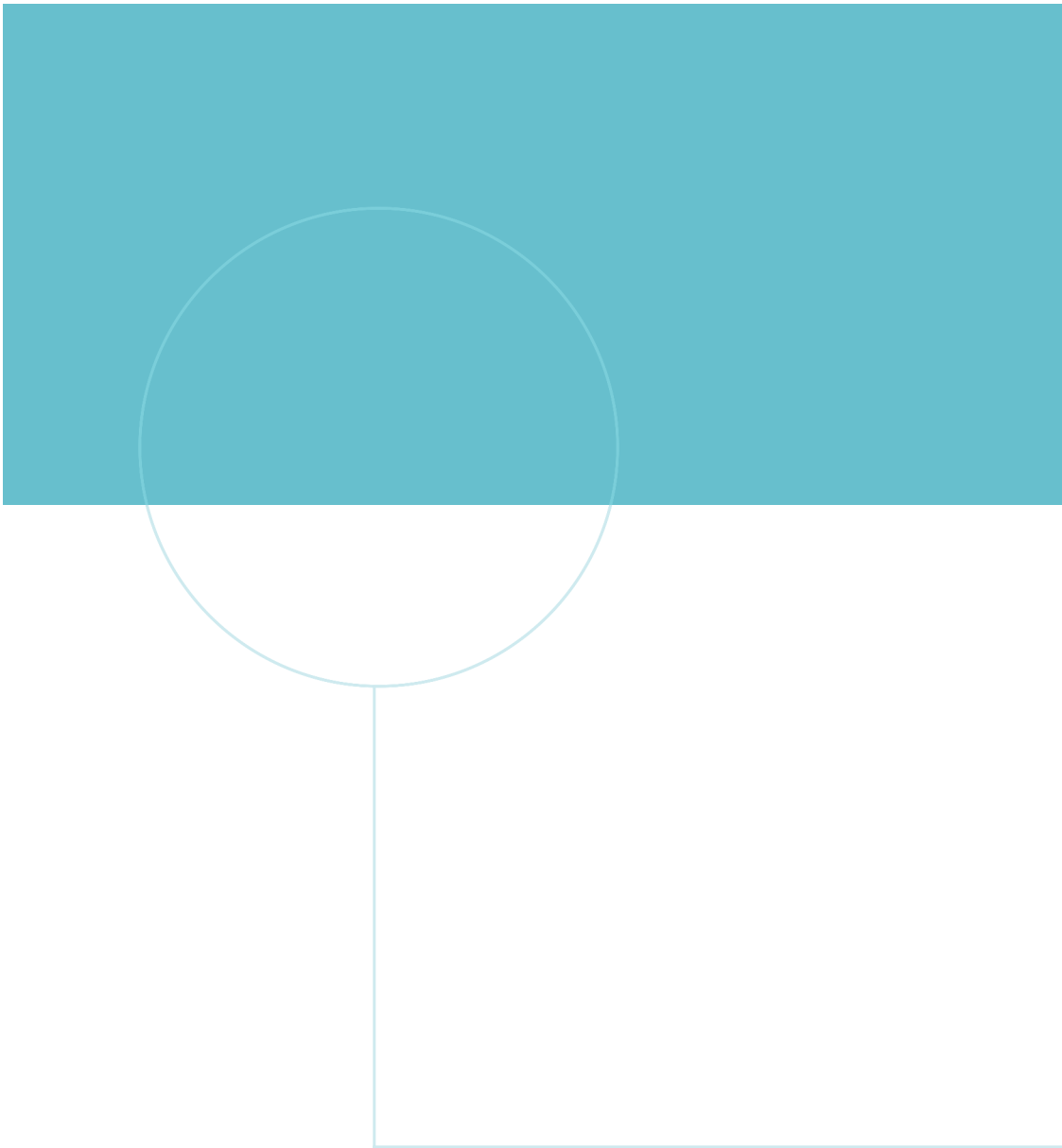

NTNU
Norwegian University of
Science and Technology